Available online at www.CivileJournal.org

Civil Engineering Journal

(E-ISSN: 2476-3055; ISSN: 2676-6957)

Vol. 8, No. 10, October, 2022

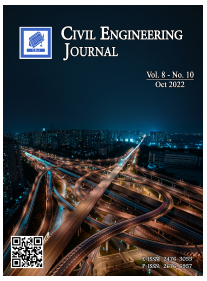

Study of Lateral Load Influence on Behaviour of Negative Skin Friction on Circular and Square Piles

Omar Shawky [1*], Ayman I. Altahrany [1], Mahmoud Elmeligy [1]

[1] *Faculty of Engineering, Mansoura University, Mansoura, Egypt.*

Received 06 July 2022; Revised 13 September 2022; Accepted 22 September 2022; Published 01 October 2022

Abstract

Negative skin friction developed on the pile surface causes many problems when piles are built in fully saturated clay. In this work, a study of NSF on a square cross-section pile corresponding to the circular pile circumference was developed. The pile was modeled as a concrete element, embedded and fully contacted with fully saturated soft clay. The clay layer is supported on a sand layer as a sub-base using ABAQUS software, and the NSF was developed on piles due to the consolidation of the clay over a 5-year period. A square pile has been found to provide lower NSF values than a round pile. Then, for the first investigation, both piles were loaded with lateral loads at the top to investigate the effect of the horizontal load on the NSF values, as there is no literature or study done on this point. The results emphasized that lateral loads reduce the NSF developed on piles. A parametric study was performed to investigate the parameters affecting the NSF values induced on piles, such as soil permeability, ballast, and lateral load values. It was concluded that square piles provide better NSF values than round piles for both single piles and pile groups.

Keywords: ABAQUS; Pile Group; Consolidation; Negative Skin Friction; Lateral Load; Drag Load.

1. Introduction

Piles constructed in soft clay were influenced by soil shear stress moving up named positive skin friction (PSF) developed on the pile surface drives the pile downward. As a result of the consolidation process, soil moves downward relative to the pile [1]. In the case of soft clay, the settlement of the soil would be greater than the settlement of the pile. Shear stress developed on the pile surface would work in down direction and caused reducing the capacity of the pile by rising the load, and the pile would be under negative skin friction (NSF) [2]. NSF results in more settlement movement of pile named pile down drag [3]. The load axially added to pile resulted from NSF becomes an extra load on the pile, defined as a drag load [4]. NSF is a process that is a function of time [5]; it goes on with the action of consolidation. NSF will influence on the piles severely [6]. Usually, piles were used in groups, not individually, so group action influenced by NSF is important to take into consideration. When piles were constructed in groups, an effect of shielding occurred. That shielding preserved protection for the inner piles, decreasing the NSF on them, and kept the outer piles subjected to a greater NSF than the inner [7].

Many types of coating were tested on piles, and it was found that a paraffin-oil mixture developed the best results in decreasing NSF when the water content was kept beneath the plastic limit value [8]. Also, it was concluded that settlement of stiffened reinforced soft clay can be reduced if the pile length was increased and pile diameter increased. The effect of the interface angle of friction was minimal [9]. When the clay soil was improved by cement, the geotechnical properties largely changed, and the preconsolidation pressure increased [10]. On the other hand, a soft clay

* Corresponding author: eng_omarshawky@hotmail.com

http://dx.doi.org/10.28991/CEJ-2022-08-10-08

mixture with cement showed a large reduction in structure settlement, and settlement can be effectively controlled by lowering the water content of the cement mix [11]. A comparison was made between circular composite pile and square composite pile and resulted in drag load developed on circular section will be more than the developed drag load on square section for composite sections [12].

Drag load was found to be totally dependent on the adjacent soil and the pile inclination angle; furthermore, these parameters can also affect the location of the neutral plan [13]. When the collapsibility of loess was checked, it was obvious that when loess downward relative to the pile, NSF would be induced along the pile surface and down drag would appear [14]. The shielding effect was responsible for lowering the drag load values on piles. Shielding effect is defined to be proportionated with the number of piles in the group (it decreased with the decrease of piles number). This paper is dedicated to studying the effect of the lateral loads of the values of the NSF induced along the pile length and the consequent drag load on both circular and square piles and pile group. An improvement of the pile cross section was made to reduce the NSF on piles, either laterally loaded piles or not laterally loaded piles, and it succeeded in reducing the NSF (97 %) [15]. This paper is considered as an extension to the study mentioned in Shawky et al. [15] to cover the effect of lateral load on the NSF behaviour. In this study, the focus was on the square piles as replacement of circular pile as they effectively reduced the NSF with approximately 60%.

2. Materials and Methods

2.1. Numerical ABAQUS Model

A 3D model will be created using ABAQUS for simulating the behaviour of the single pile and pile groups. The piles were assumed to be in complete contact with the adjacent soil. In this study, two types of elements (C3D8R and C3D8RP) were used to simulate concrete piles and soil, respectively. These elements are the 8-node reduced integration with hourglass control quadratic element, the 8-node tri-linear reduced integration displacement, and the pore water pressure quadratic element, respectively [16].

2.2. Contact Elements

The ABAQUS software is able to create a contact element with thickness = zero between the interface of the previous two elements to allow the creation of the frictional stress between the pile surface and the soil. The software used the theory of Coulomb friction, which specified the friction response by determining the friction coefficient at the interface with the value of the displacement limit (critical) with the displacement value of the shear = 5 mm to achieve the status of the interface friction motion, as shown in Figure 1.

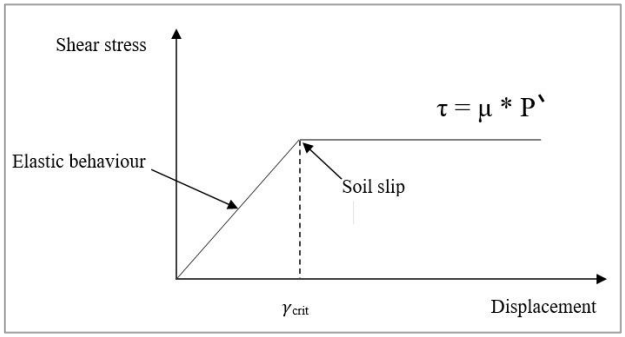

Figure 1. Performance of interface element [17]

2.3. Boundary Conditions

For the vertical sides of the model, they should be allowed to move vertically but not horizontally, so the boundaries should be considered fixed in the horizontal direction and the vertical direction will be free. For the bottom of the model, it is not allowed to move in any direction, so the boundaries at the bottom will be considered fixed, both vertically and horizontally.

2.4. Constitutive Models

Cam-clay model was used to simulate the behaviour of soft clay. The model was designed to simulate the characteristics of normally consolidating clay. The model was induced for completely saturated clay, and the stress value is the defined effective stress. Also, the Cam clay model has the capability to compute the soil volumetric change that will appear due to the consolidation process. For the bearing layer, the Mohr-Coulomb model was used to simulate the behaviour of the sand soil located beneath the clay soil to support the pile tip. It is one of the most powerful models that uses the elastic – perfectly plastic concept to represent such soils with acceptable accuracy and easy to use with few parameters [18].

2.5. Analysis Methodology

The model was built for single pile in soft clay with surface surcharge loading to start the consolidation process. Due to consolidation and excess pore water, soil will move downward and relative displacement between the pile and soil will take place, then NSF will be generated on the pile surface. The aim of the study is to investigate the effect of lateral loads on NSF and study the ability of decreasing the NSF by replacing the circular pile with square pile with equivalent perimeter (see Figure 2).

- In the beginning a circular pile was constructed as reference pile to compare all the results relative to this pile. The NSF will be generated on the pile due to soil settlement relative to pile according to consolidation process;
- A square pile with equivalent perimeter (perimeter of circular pile) and compare the NSF values with the NSF developed on reference pile;
- Lateral load was added at the top of circular pile and calculate the NSF compared to the NSF developed on the circular pile without lateral load (reference pile);
- Lateral load was added at the top of square pile and calculate the NSF compared to the NSF developed on the square pile without lateral load;
- Parametric study was made with different values of soil permeability as permeability influence the excess pore water from soil and soil settlement. Then surcharge loading because it represents the main factor of consolidation process due to pressure on soil. After that the interface friction coefficient between soil and pile was investigated. The lateral load value to detect the effect of increasing of lateral load value on the value of NSF, and eccentricity of pile as it is important case for laterally loaded piles. Finally compare the results for circular and square piles to determine the most suitable type to reduce the NSF on pile surface.

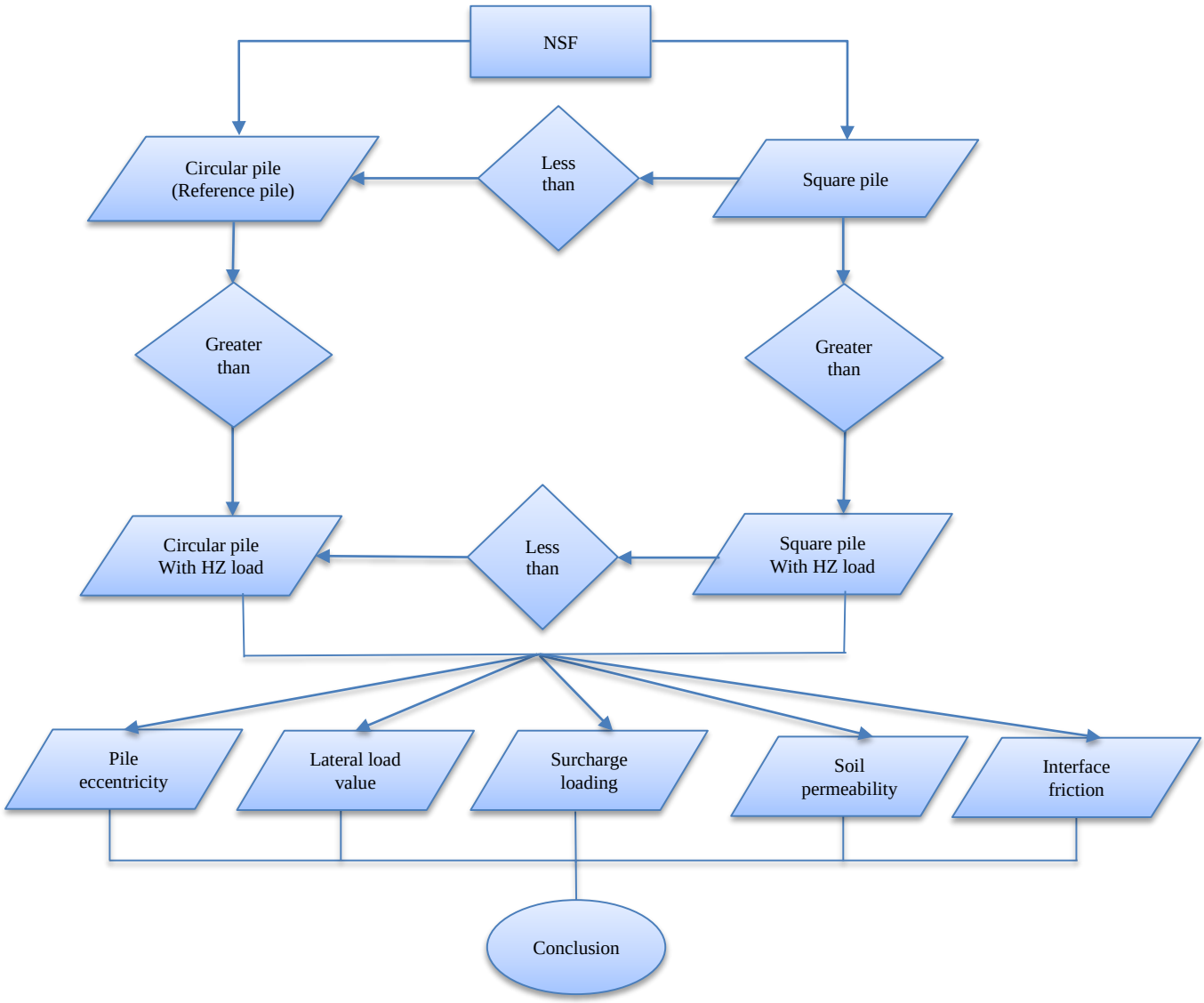

Figure 2. Flow chart of analysis methodology

3. Analysis of Circular Pile Not Subjected to Lateral Load

This study is performed on a circular concrete pile with a diameter (D) = 500mm. The pile length (L) is assumed to be 20.0 m. It should be built up in a fully saturated, consolidated, soft clay layer. The pile is modelled in full contact with the surrounding clay soil. At the bottom of the soft clay below the pile tip, the supporting sand layer starts as supporting soil and with a depth (depth = 0.7 l) that gives depth (depth = 14.0 m) for the sand layer. These dimensions give a total bottom depth = 34.0 m. To give the half width of the model (W) assume (W = 25 pole diameters) which gives (W = 12.5 m) giving a total width of 2 W = 25.0 m results in Randolph and Wroth [19]. The full geometry of the model is shown in Figure 3. The surface load is 50 kN/m^2 evenly distributed over the entire surface. The water level was assumed to be at ground level. This leads to consolidation of the soil as a result of soil self-weight and surface load distributed on the surface and as a result of NSF and downward resistive loading along the pile surface. The solidification time (T) is assumed to be 5 years to allow the soil to settle and NSF to occur.

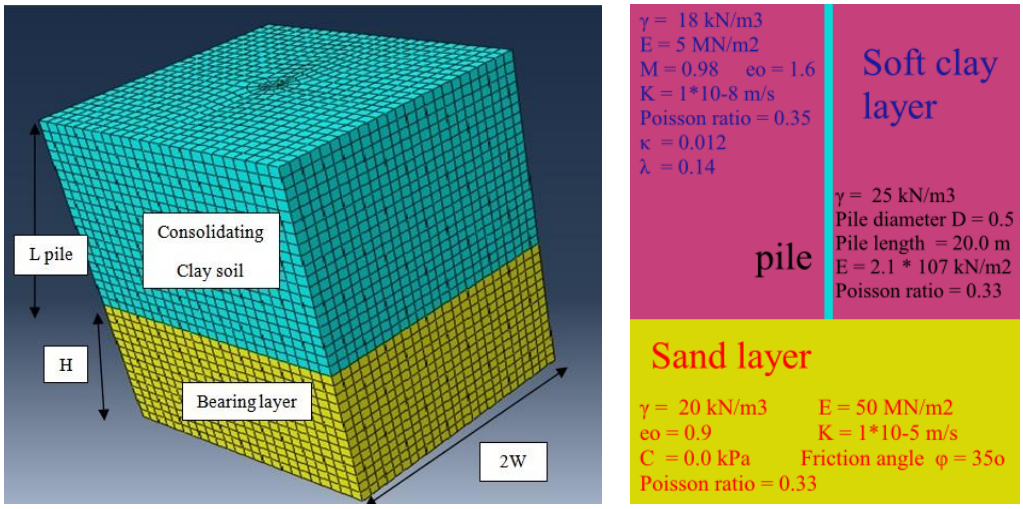

Figure 3. Dimension of model and properties of soil and pile [20]

The model was executed to compute the NSF and the drag-load on the pile at the completion of the consolidation process. The results of this pile should be taken as the guide line to be compared with new piles.

Figure 4 presents the skin friction distribution along the pile length. The Upper part of pile is subjected to NSF stress downward and denoted by (–ve) sign this is due relative displacement between soil and pile as shown in Figure 5 where soil settlement is greater than the pile settlement. Shear stress varies with increasing rate till reach maximum value then it decreases to reach zero stress value. The skin friction turns to the other side and changes to PSF around the lower part of the pile and denoted by (+ve) sign continues to the tip of the pile. This point of zero shear stress location determines the position of neutral plan which located at the point which there is no relative displacement between soil and pile at (Z/L = 0.86). Beneath the neutral plan location, the pile settlement will be larger than soil settlement and the shear stress changes its direction upward developing the PSF. The point of zero shear stress is placed at the resultant location of pile-soil interaction to the force equilibrium which states that the NSF will be in balance with the unit pile PSF.

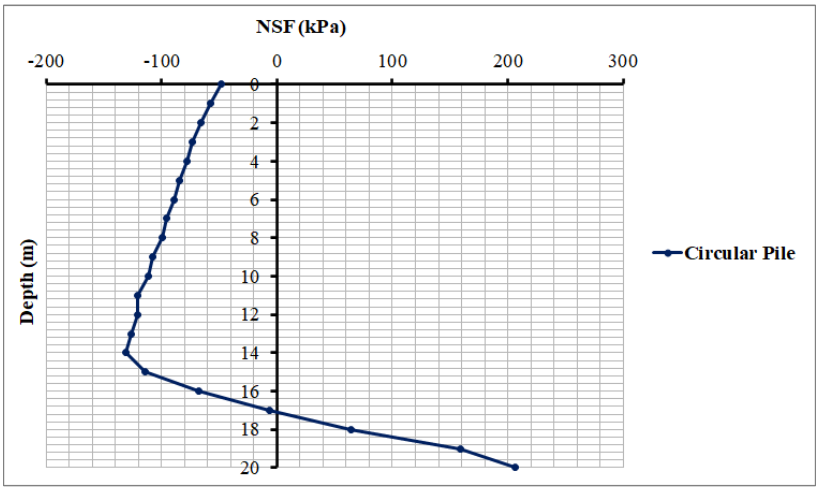

Figure 4. Distribution of NSF along pile length and location of NP

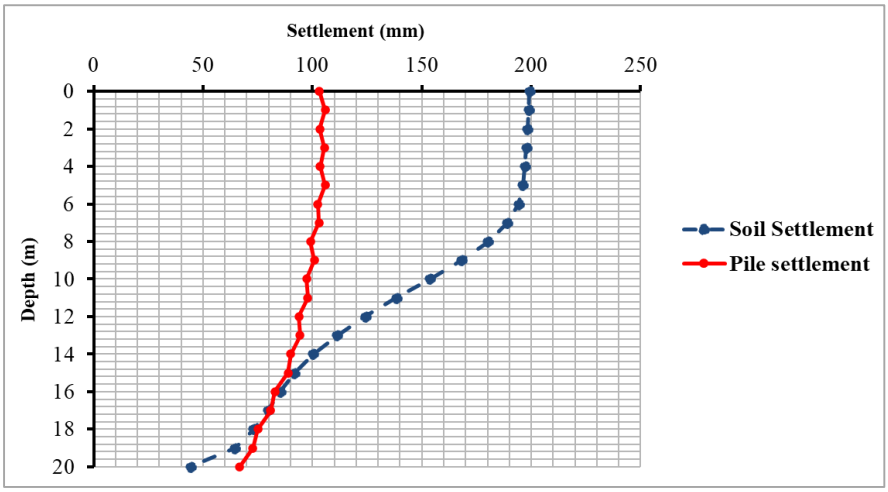

Figure 5. Settlement of pile and soil

Figure 6 shows the distribution of the drag load on the pile surface. The drag-load has an acceptable agreement with the expected distribution as it increases at the top part of the pile and decreases beneath the neutral plan location. Drag-load is the summation of the NSF stress on the pile while the entire resistance of the pile is the summation of positive pile resistance. This condition of balance of stress determines the place of the neutral plan.

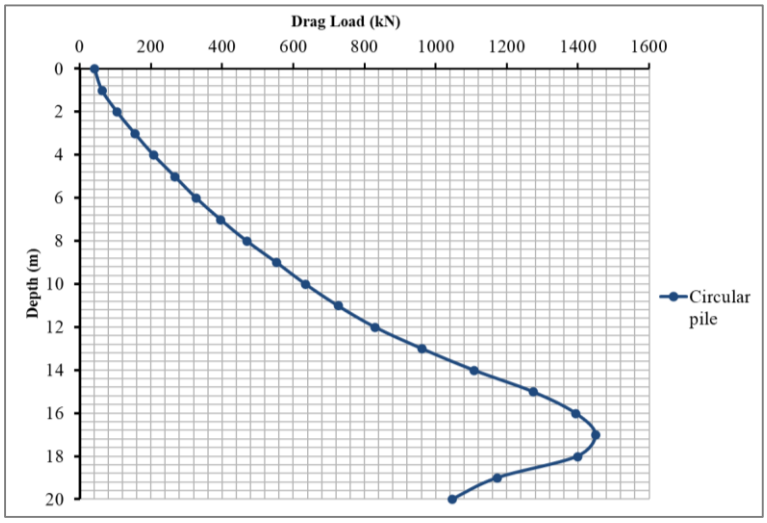

Figure 6. Drag load distribution along the pile surface

4. Analysis of Circular Pile Subjected to Lateral Load

Second model will be executed to investigate the influence of the lateral load on the value of NSF developed on the pile. The horizontal value was chosen to be (10 kN) acting at the top of pile. Same pile parameters and model geometry were used.

Figure 7 illustrates the distribution of NSF along the pile length due to side loading of the pile at the top. The calculated NSF distribution along the pile shows a sharp reduction in NSF values from the top of the pile to a depth of 5.0 m. The values are very small, approaching zero, then gradually increasing to achieve the maximum NSF value which is less than 28.5% of the maximum NSF of the pile under consolidation surcharge load only with no lateral loading. This result was consistent with the prediction inferred from the pile and soil settlement in Figure 8. The reduction was a result of the lateral drag of the soil developed due to lateral loading and the increase in soil stress. It is known that the reaction process in horizontally loaded piles is to transfer the horizontal load to the surrounding soil through the lateral resistance of the soil, as shown in Figure 8. When the top of the pile tries to move in the horizontal direction when the load is applied. This caused a bending moment and rotation or complete displacement of the piles. The piles will compress the soil in front of their surface in the direction of loading, creating compressive stress and shear stress within the soil that would create resistance to pile displacement. This gives the condition of equilibrium between the applied horizontal loads versus the soil resistance induced on all pile faces (Figure 9). The curve showed that the effect of horizontal loading continues along the pile surface to a depth of 4.0 m. then it gradually decreased, after which the value of NSF began to increase.

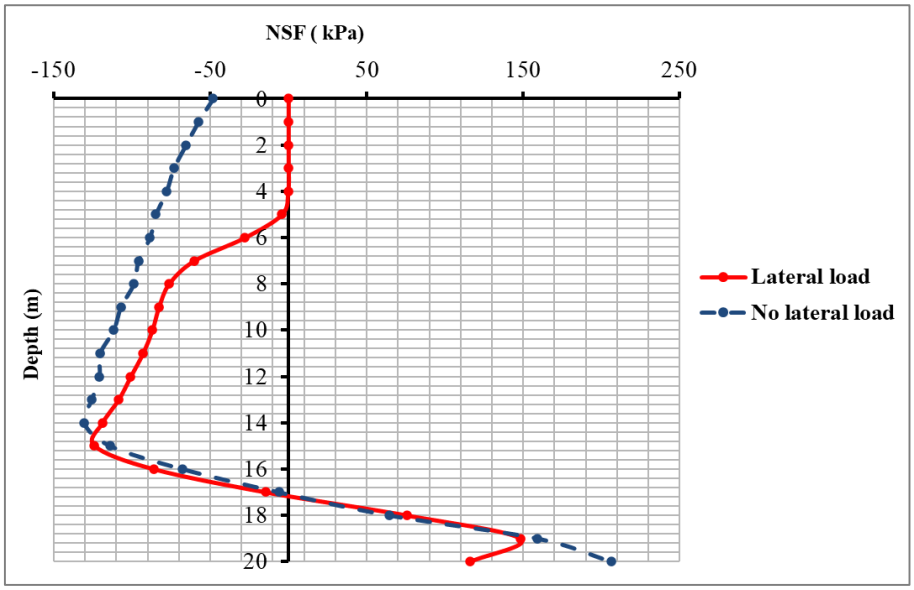

Figure 7. Distribution of NSF on circular pile with horizontal load compared to NSF distribution without horizontal load

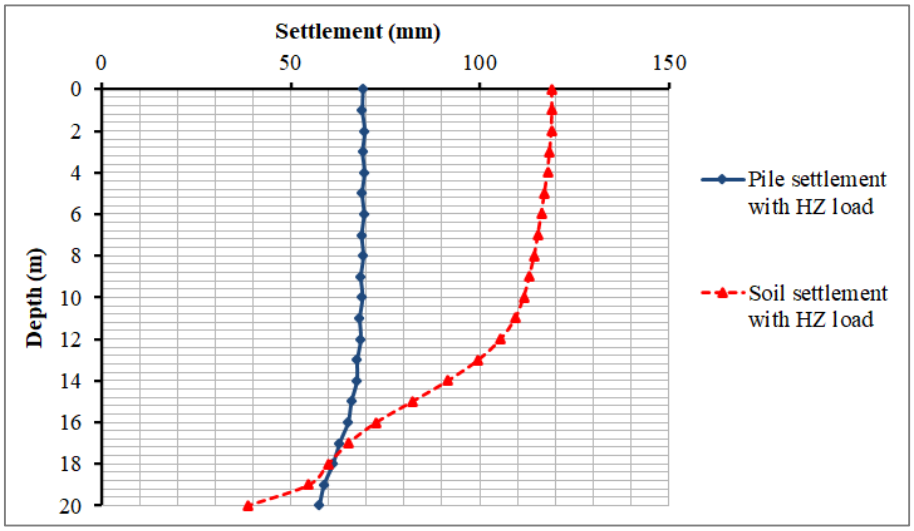

Figure 8. Settlement of pile and soil with lateral load

The result of the drag load illustrated that a reduction of 35% of the maximum value of drag load was developed on the pile due to the influence of horizontal load at the pile top and a complete reduction of the values of the drag load along the pile surface from the top till tip. The resulted drag load showed an agreement with the prediction concluded from settlement.

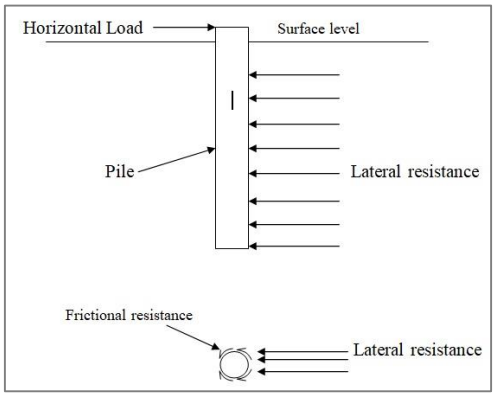

Figure 9. Soil resistance of lateral load on piles

Figure 10 shows the distribution of drag load along the pile surface. Settlement of pile is shown in Figure 11 as appears in ABAQUS model.

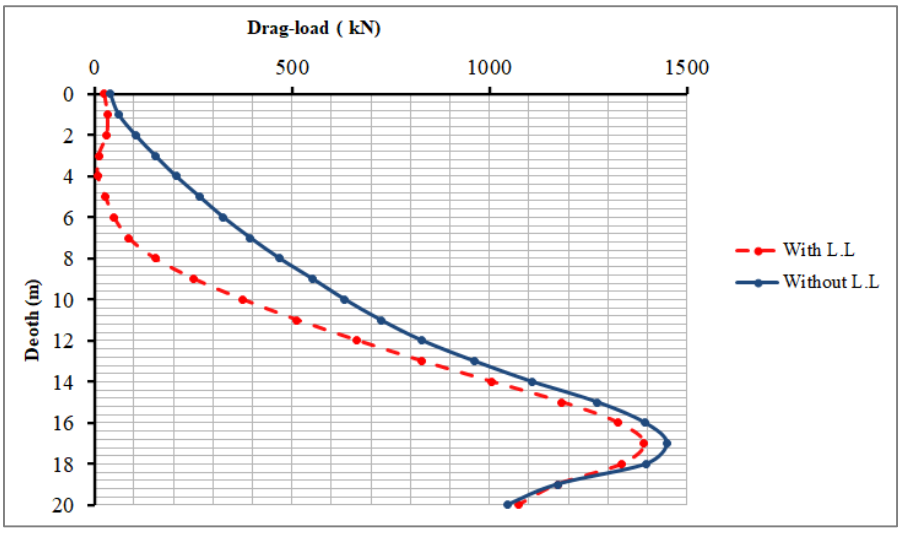

Figure 10. Drag load distribution along the pile surface with and without lateral load

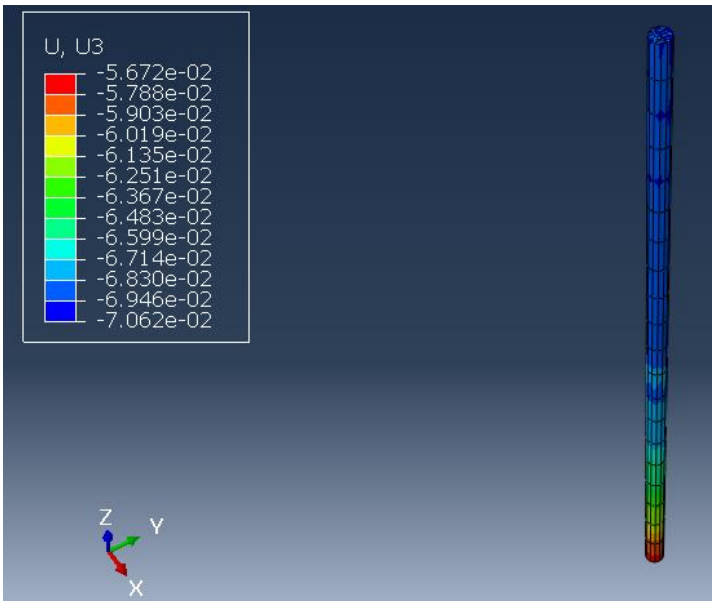

Figure 11. Contours of settlement of pile

5. Analysis of Square Pile

A new model was created to simulate a square pile with equivalent perimeter to the circular pile. The side length was taken 40 cm to give the same pile surface area in contact with soil. The model used same parameters and load values applied on the circular pile model. The pile was subjected to lateral load 10 kN at the top to investigate the behavior of the square piles compared to circular ones (Figure 12). Figure 13 shows the distribution of NSF on square pile compared to the circular pile.

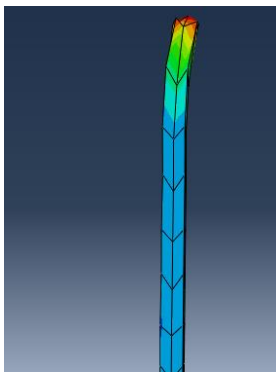

Figure 12. Lateral displacement of square pile subjected to lateral load

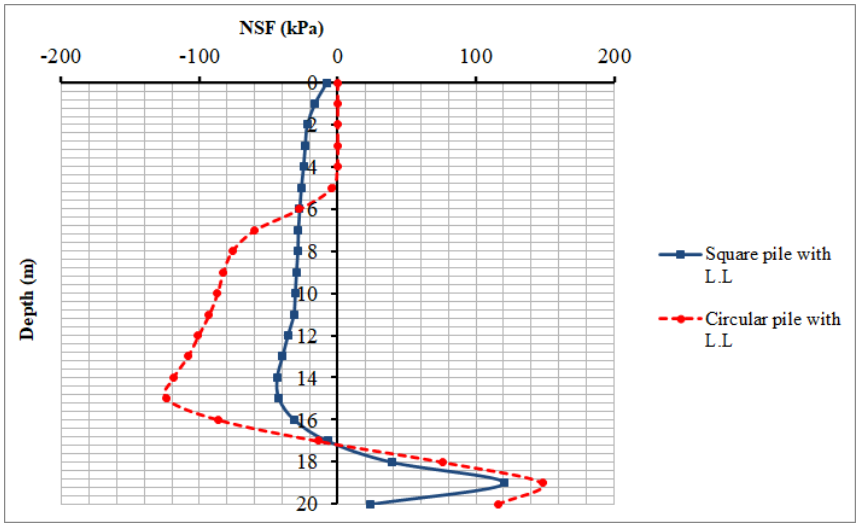

Figure 13. NSF distribution along square pile compared to circular pile

It is clear that maximum value of NSF for square pile is less than NSF developed on circular pile. Circular pile provided better behaviour at the top of pile where the NSF is approaching to zero at the first 3 meters then it was gradually increased due to the action of horizontal load on the pile. In the case of the square pile the behaviour of NSF on the pile surface did not have been influenced by subjecting to horizontal load. Geometry of pile plays big role in this result (shape effect) as when circular pile is subjected to horizontal load. The maximum soil shear in the front side will be formed in the centre and decreased while moving to sides while decreasing longitudinally downward till the effect of horizontal load vanishes according to the pile lateral displacement. On the contraire of square pile, the maximum soil shear will be constant all over the surface as shown in Figures 14 and 15.

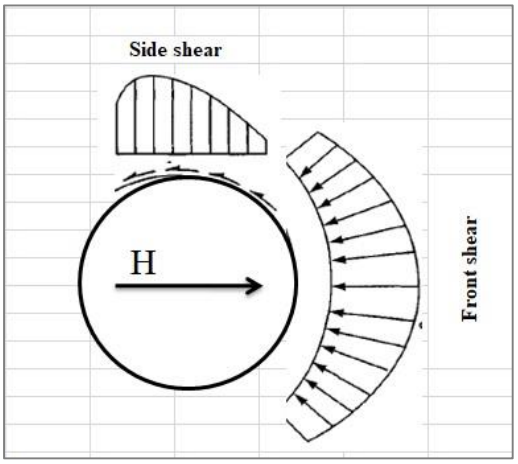

Figure 12. Distribution of lateral soil shear on circular pile subjected to horizontal load

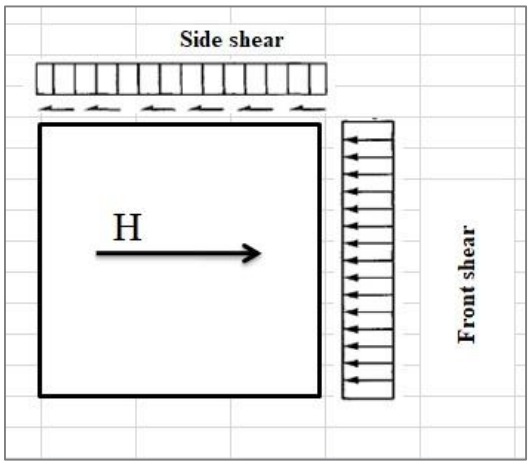

Figure 13. Distribution of lateral soil shear on square pile subjected to horizontal load

Figure 16 showed the drag load distribution on the square pile surface versus the circular pile. It was observed that the value of the drag load of square pile is 10.5 % less compared to the circular pile under horizontal load. This result agrees with computed NSF previously Figure 13. The NSF distribution of the square pile was largely influenced due to the existence of horizontal load on the pile and the values were more than the circular pile on the top 6.0m of pile. Then the maximum NSF was reduced from this point to be less than the NSF developed on the circular pile to reach about (73.3 % less). It is clear from these findings that square piles provide better behaviour for developed NSF under lateral loads.

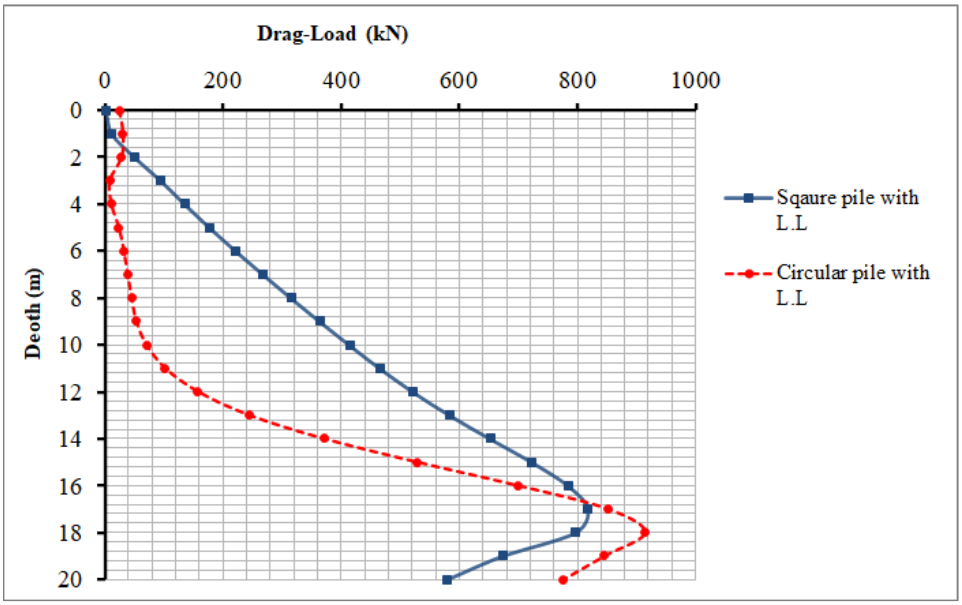

Figure 14. Distribution of drag load along circular pile compared to square pile subjected to horizontal load

6. Parametric Study of Pile Group

Two sets of pile groups were created. The size of group is 3x3 piles. First set is circular pile group and the second one is square pile group to compare the NSF behaviour on the pile groups when the piles are subjected to lateral loads. Piles in the group will be classified as Corner pile, edge (side) pile, and centre pile as shown in Figure 17. The distance between the piles is three times the diameter of the piles (3D = 1.5 m).

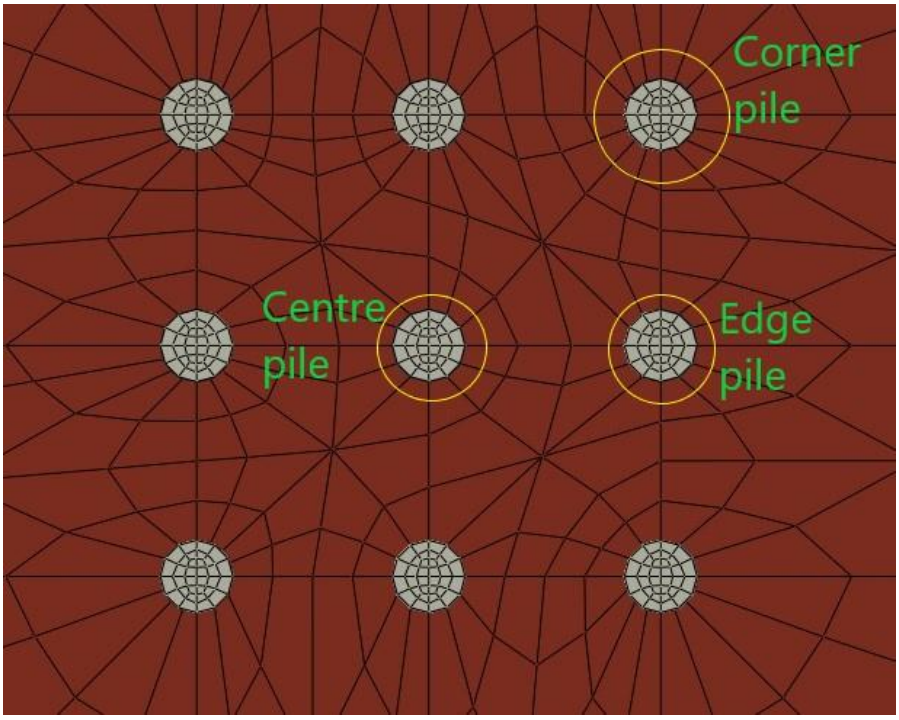

Figure 15. Classification of piles in (3×3) group

When piles are subjected to lateral loads an interference of stress zones were formed in soil due to the movement of piles and progressive transformation of lateral displacement. This interference of stress resulted in some piles were affected more than others in addition to the grouping action of piles NSF on piles may show impressive behaviour (Figure 18).

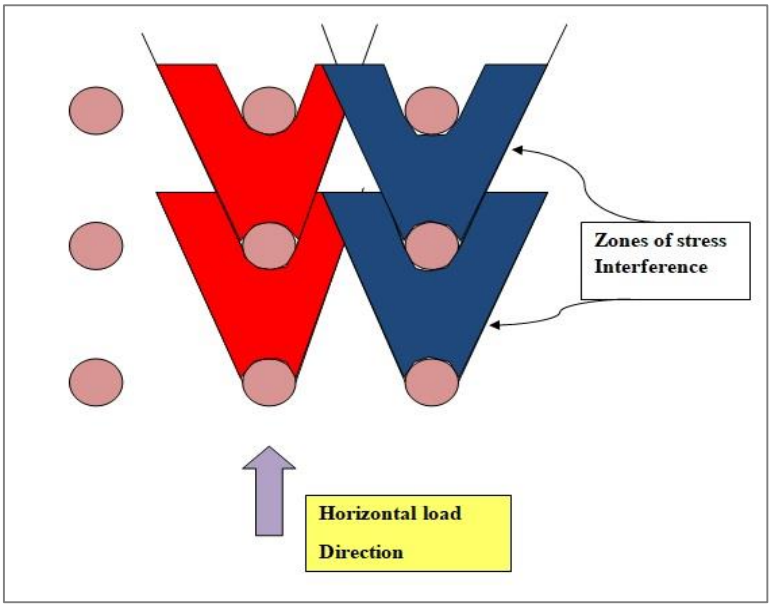

Figure 16. Interference of stress due to horizontal load on piles

6.1. Influence of Interface Friction Coefficient (μ)

Models were executed to simulate the behaviour of soil when the interface friction coefficient between soil and pile surface was changed to take values of 0.1, 0.2, 0.3, and 0.4 (Figure 19) [21]. Both cases of circular piles and square piles were modelled and results are presented to compare each position of circular pile in the circular group sized (3×3) with the synonymous square pile in the square group with size (3×3).

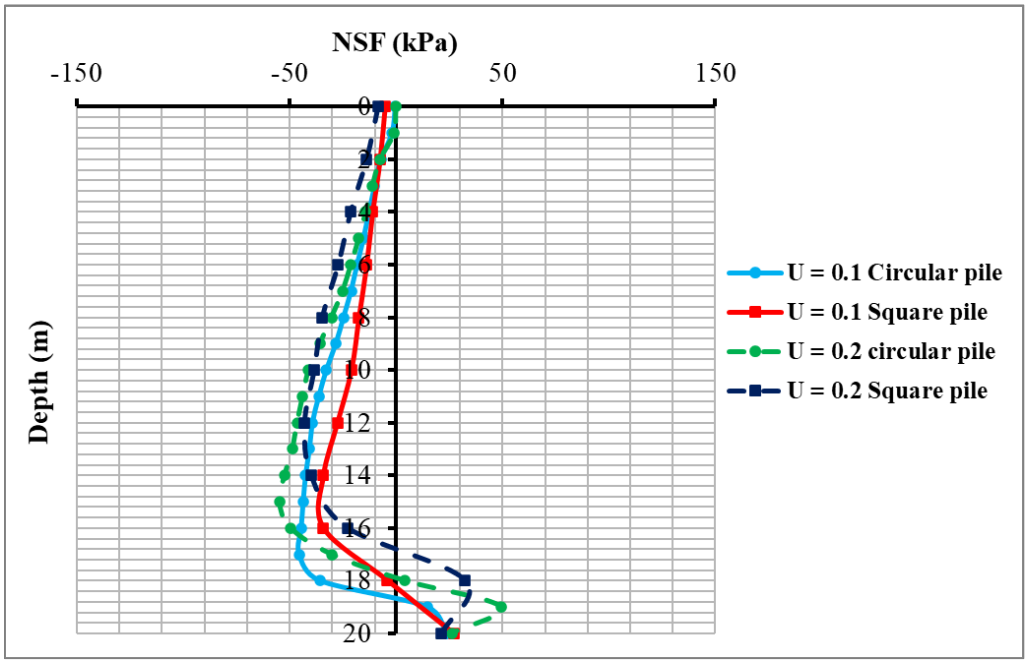

Figure 17. Distribution of NSF along Corner circular pile compared to Corner square pile in group size (3×3)

Results of analysis indicated that for both circular and square piles when subjected to lateral loads NSF developed on pile surface changed proportionally with the interface friction coefficient. It increased with increase of (μ) as it is known that shear stress value is depending on friction coefficient ($\tau = \mu\sigma$) and (σ) is the normal effective stress between the contact surfaces (Figure 20).

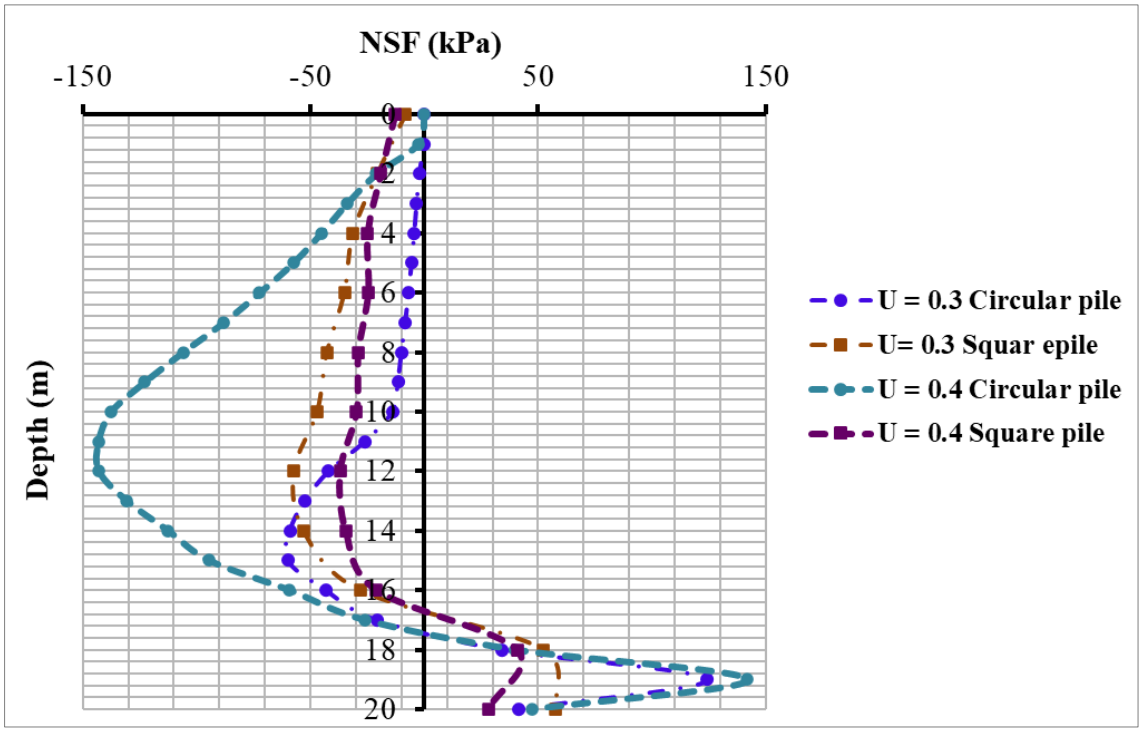

Figure 18. Distribution of NSF along Corner circular pile compared to Corner square pile in group size (3×3)

Also, the results illustrated that square piles provided NSF values less than the induced NSF values on circular piles. These findings were consistent with the results of single piles shown previously illustrating that behaviour of square piles was better than circular piles when developing NSF under the action of lateral load. Comparison between the results of corner piles, edge piles, and centre piles clarified that NSF was decreasing on both circular and square piles according to their position in the group. The maximum values were developed on the corner piles then decreasing on the edge pile and the minimum value was generated on the centre pile. This behaviour was predicted to appear due to the grouping action (shielding action) on piles as the perimeter piles sheltered the inner piles (Figure 21 to 25).

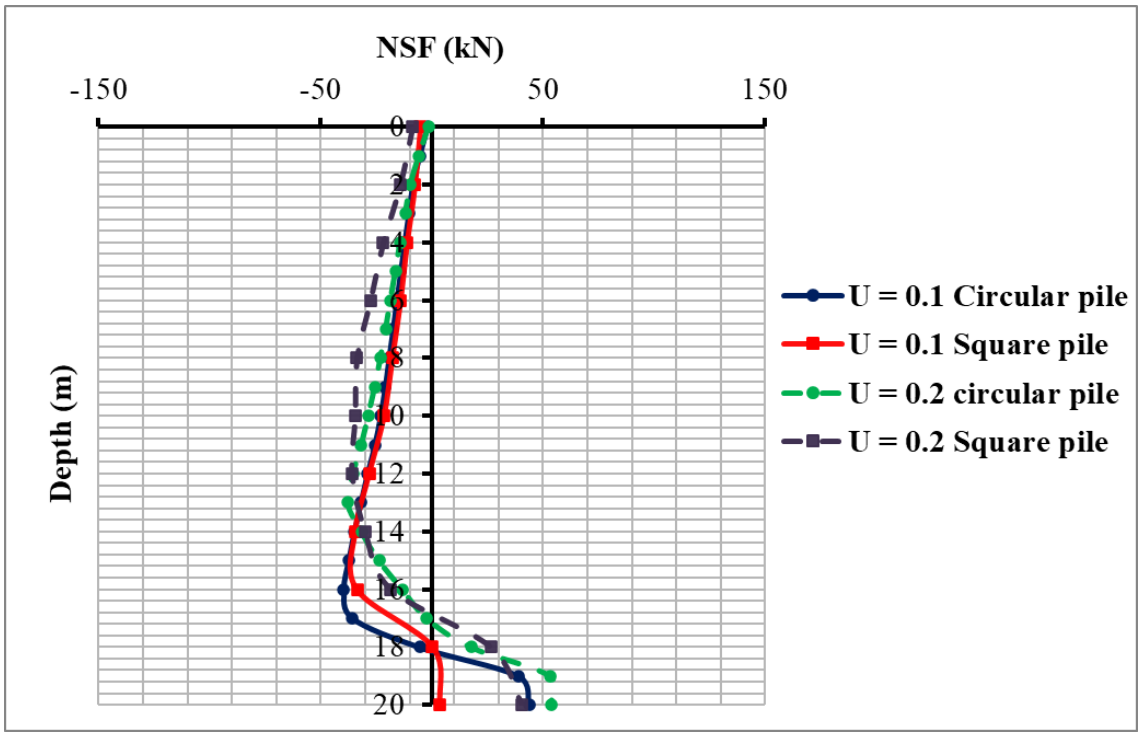

Figure 19. Distribution of NSF along Edge circular pile compared to Edge square pile in group size (3×3)

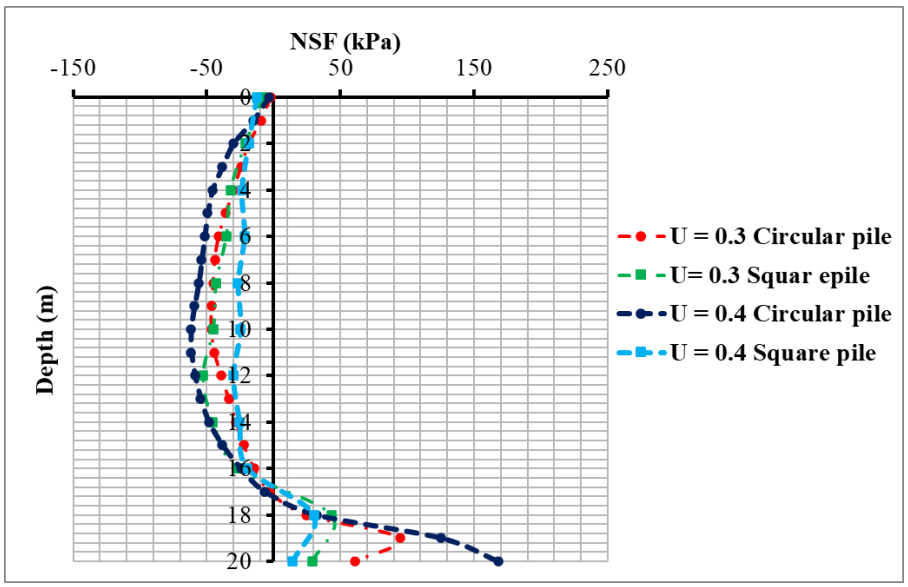

Figure 20. Distribution of NSF along Edge circular pile compared to Edge square pile in group size (3×3)

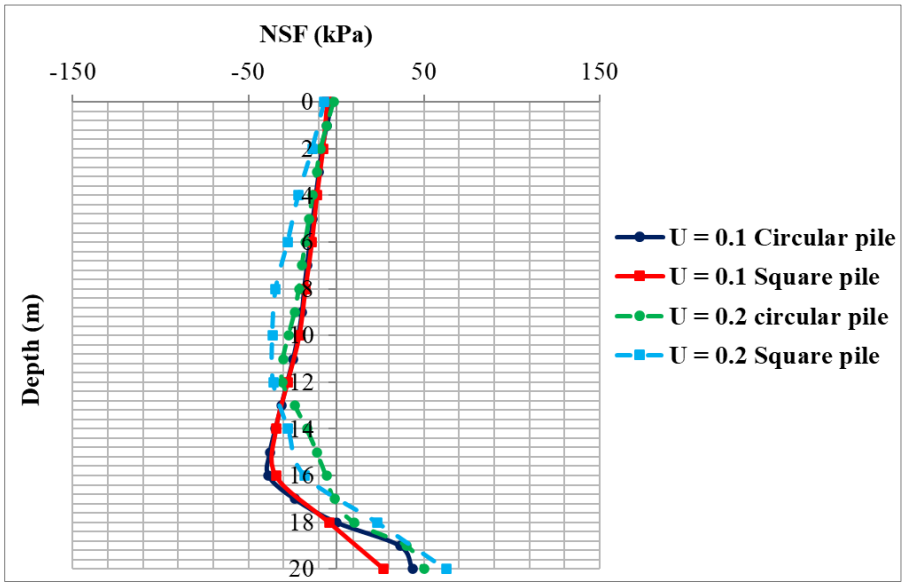

Figure 21. Distribution of NSF along Centre circular pile compared to Centre square pile in group size (3×3)

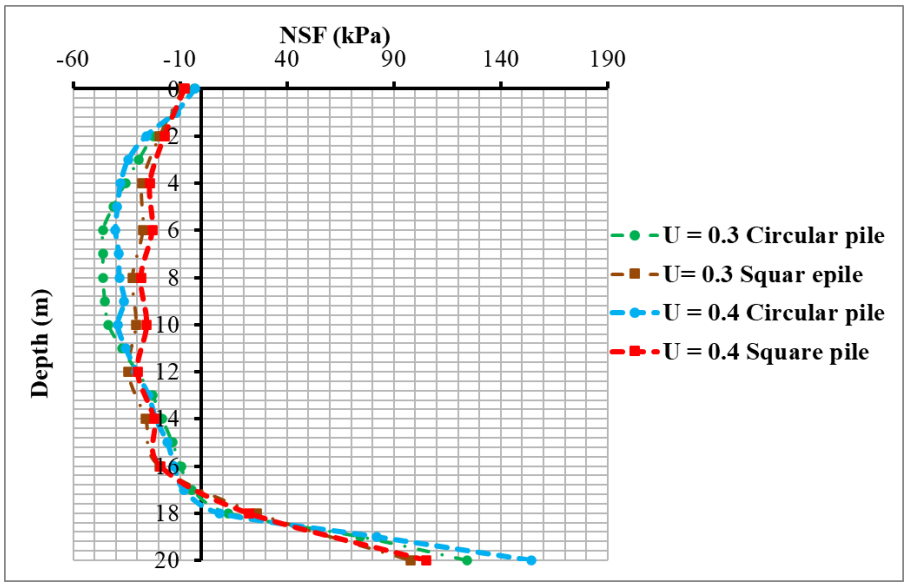

Figure 22. Distribution of NSF along Centre circular pile compared to Centre square pile in group size (3×3)

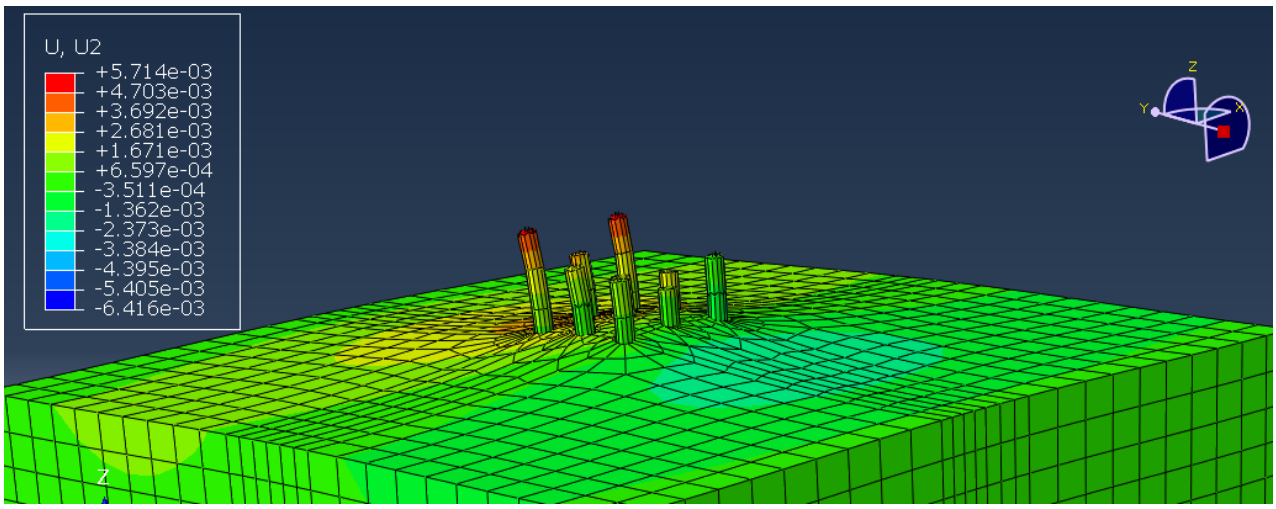

Figure 23. Lateral displacement of square pile group size (3×3)

6.2. Influence of Changing Soil Permeability (K)

Permeability depicted a major aspect of the consolidation process. It determines the velocity of the excess pore water from the clay layer. It is known that permeability decreases when confining pressure increased. Additional models were executed to investigate the behaviour of soil when the clay permeability changed. Permeability of soft clay can take any value in the range from (1 E-9 to 1 E-7 m/s). The common values of permeability to be used as found in site of construction varies from (0.5 E-8 to 1.2 E-8) [22]. Other values of permeability were suggested in this search below (0.5 E-8) and above (1.2 E-8) to study the entire range of permeability effect on NSF values when the piles are subjected to lateral loads.

10 models of individual circular piles were created with 5 different values of permeability for the same consolidation time 5 years and same surface surcharge 50 KPa. The lateral load on the pile is kept to 10 KN. Results of NSF for the single piles are shown in Figure 26.

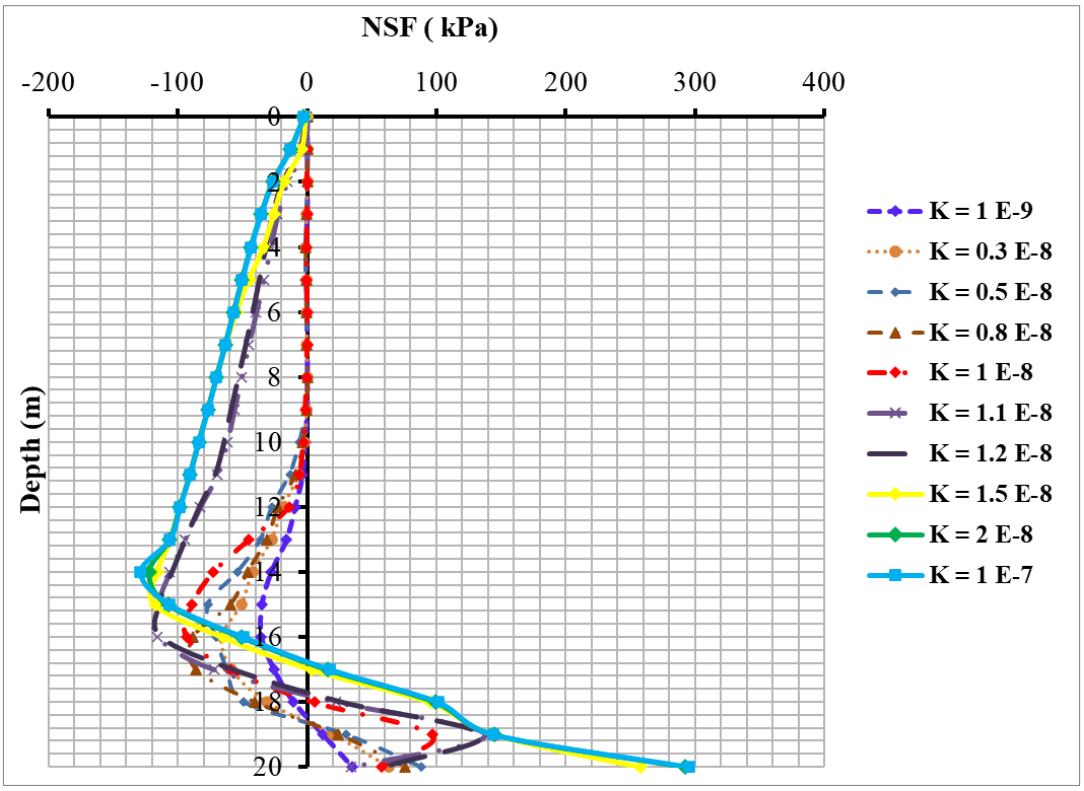

Figure 24. NSF distribution along single circular piles for different values of permeability

Figure 26 showed the distribution of NSF with different permeability coefficients. With the expansion of coefficient of permeability, the developed NSF increased. The minimum NSF was (-88.1 kPa) and the maximum was (-120.1 kPa)

with difference (32 kPa). The NSF increased with the increase of the coefficient of permeability but the lateral load influence on the piles was noticed to be large on the piles with small permeability. Results showed that at the top of piles the NSF was extremely small (zero in some points) then the NSF increased till reach its maximum value. The reason of this result is that when the permeability increased the soil settlement due to consolidation increased which consequences in increase the relative displacement between soil and pile.

From the curve it was shown that the influence of the horizontal load decreased with the increase of permeability coefficient. In the first 5 results the influence of horizontal load started to decrease near the mid pile while in the other 2 results it decreased very much earlier. That behaviour may be due the more ability of soil to keep water inside particles for the small permeability coefficients which made it quite smooth for the pile to impact on soil while when the permeability increased the soil tended to be stiffer and the lateral impact decreased more recently. The NP location was noticed to be moving upward with the increase of the permeability coefficient which produced a reversal correlation between the value of the permeability and the location of NP on the pile.

The same investigation was repeated for the square piles subjected to lateral loads for all values of permeability. Figure 27 displayed the NSF distribution along the square individual piles for the different values of (K). It could be observed from the computations that NSF values developed in soils with coefficient of permeability that was less than (1 E-8 m/s) have significant difference (20 kPa). While NSF values induced in soils with permeability coefficient greater than (1 E-8 m/s) were almost equal which leads to deduce that permeability has limit in affecting the developed NSF. This limit was reached at (K = 1.1 E-8) and all other values more than that will not cause significant change. In addition, when compare the values of NSF of circular piles and square piles observations clarified that for ($K \leq 1$ E-8) square piles provided better behaviour than circular piles for the same values. But for (K > 1 E-8) circular piles and square piles have approximately similar behaviour and the difference between them can be ignored. This matched reaction of both piles to the increase of permeability may be due to the increase of soil settlement and the relative displacement between pile and soil while geometry of pile did not influence the NSF values.

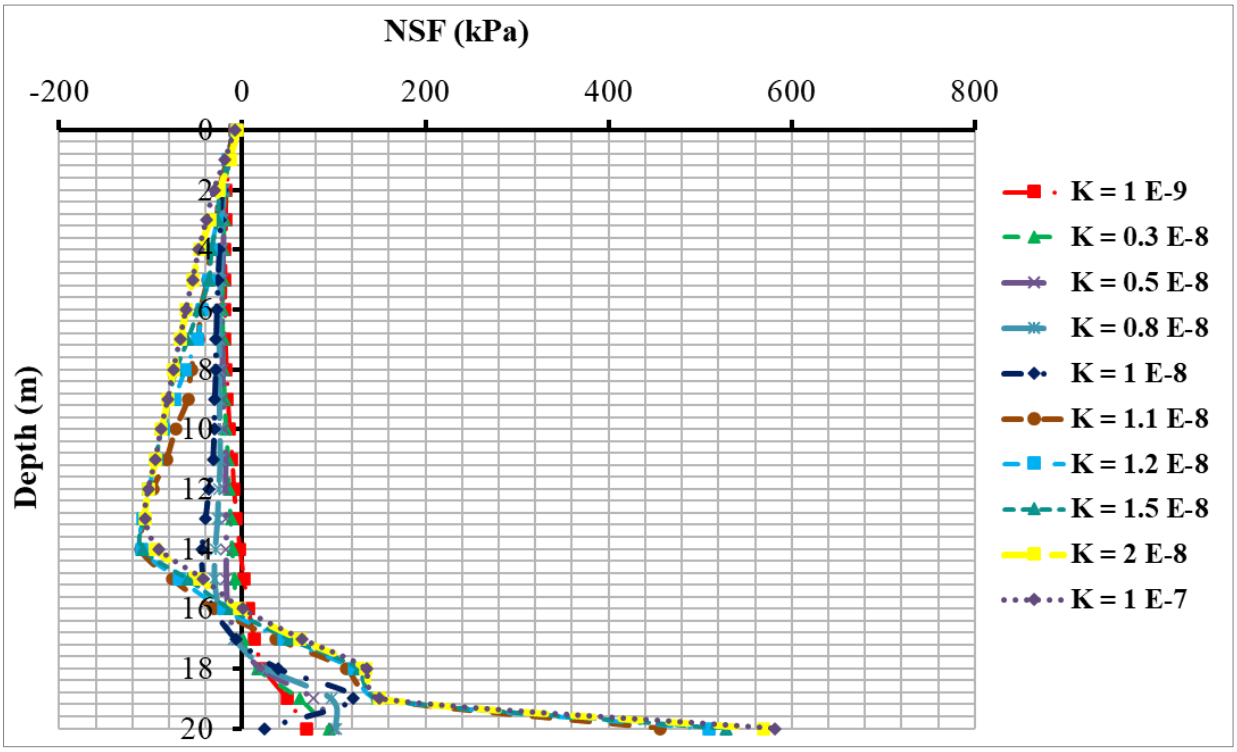

Figure 25. NSF distribution along single square piles for different values of permeability

For the pile groups the group sized (3×3) was modelled to present circular pile groups and square pile groups using all values of soil permeability (K). The following Figures illustrated the results comparing each pile in the group of circular groups with its match in the square groups for few selected values of (k).

Results shown in Figures 28 to 33 indicated that corner piles in both shapes of piles developed the larger NSF, centre piles induced the less NSF, and edge piles have intermediate values of NSF that are less than corner piles and larger than centre piles. This behaviour agreed with the grouping action which formed shielding effect around the centre pile which has the maximum shielding effect.

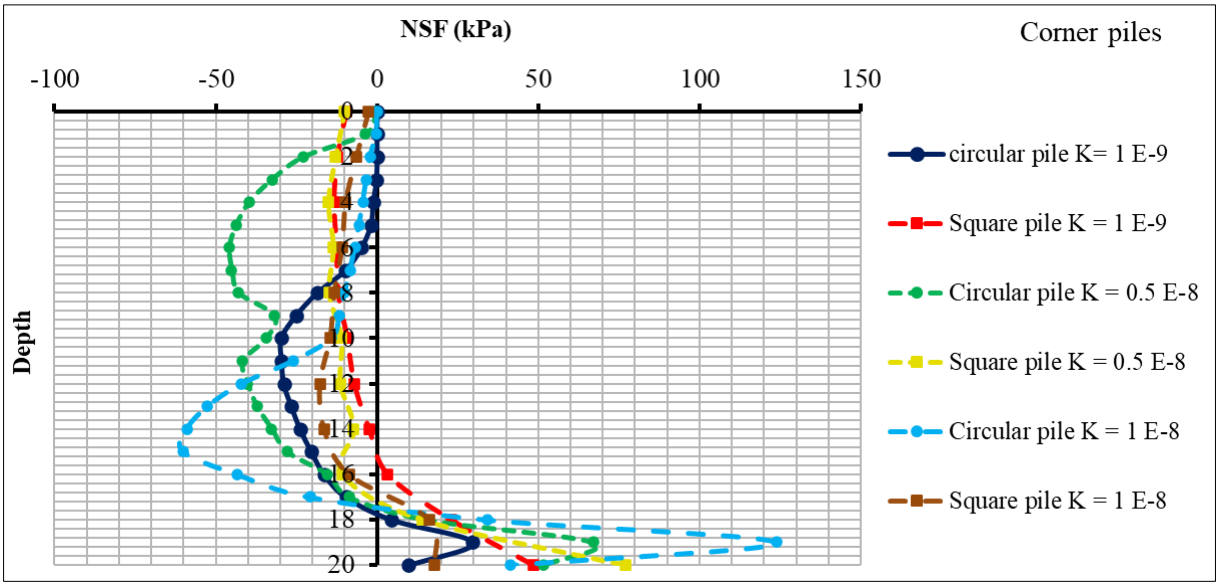

Figure 26. NSF distribution along corner circular piles compared to corner square piles for different values of permeability

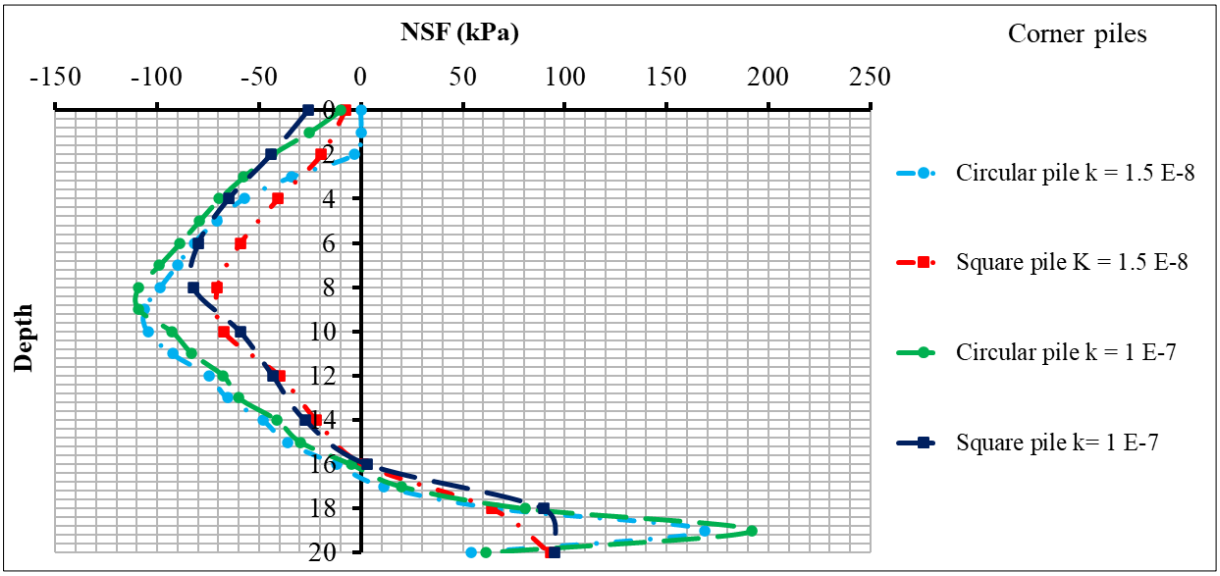

Figure 27. NSF distribution along corner circular piles compared to corner square piles for different values of permeability

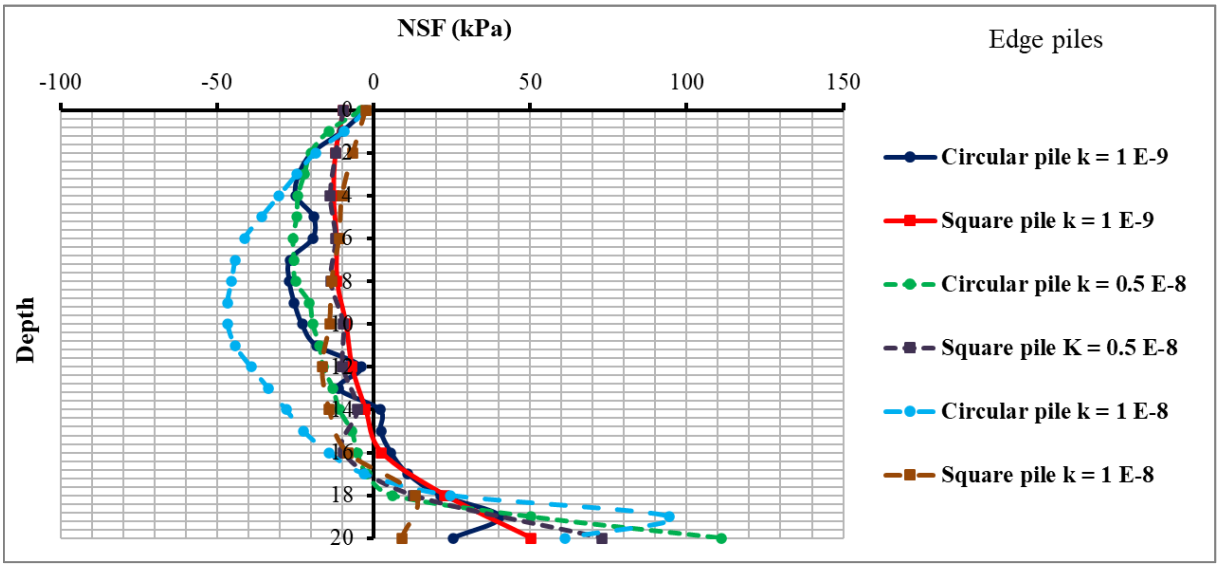

Figure 28. NSF distribution along edge circular piles compared to corner square piles for different values of permeability

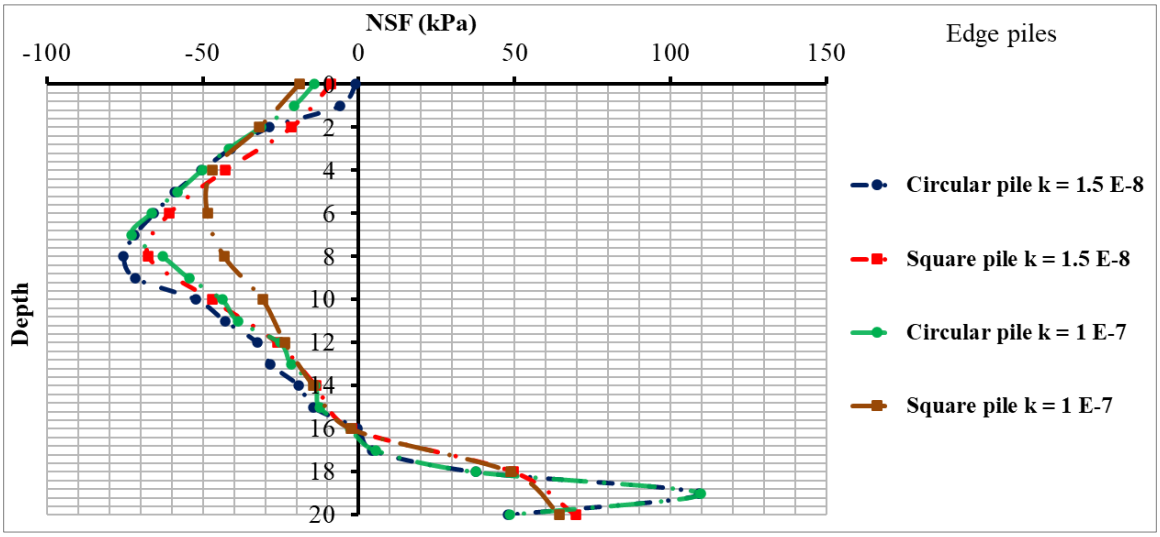

Figure 29. NSF distribution along edge circular piles compared to corner square piles for different values of permeability

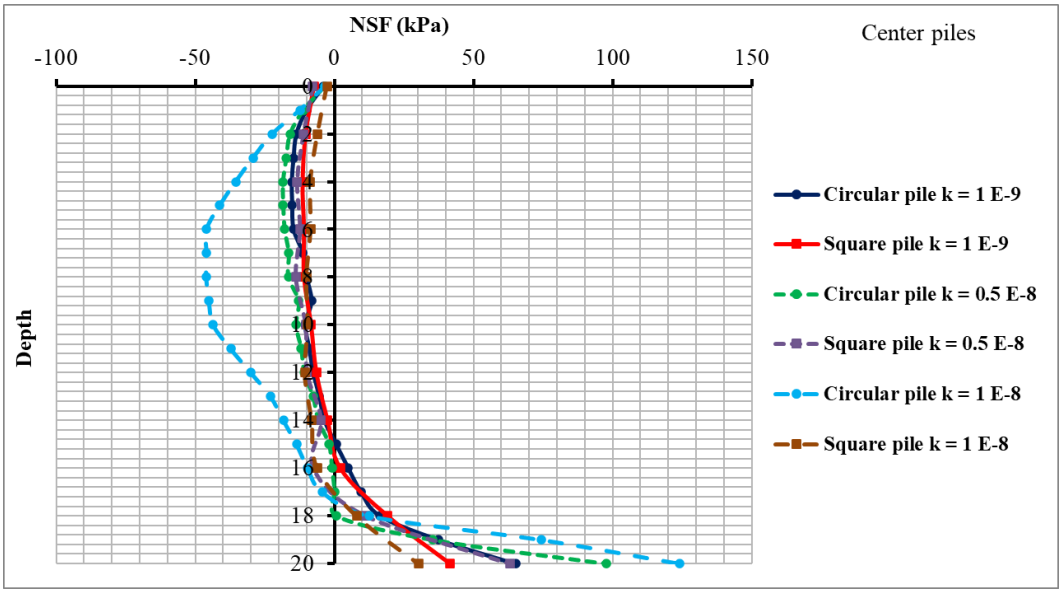

Figure 30. NSF distribution along centre circular piles compared to corner square piles for different values of permeability

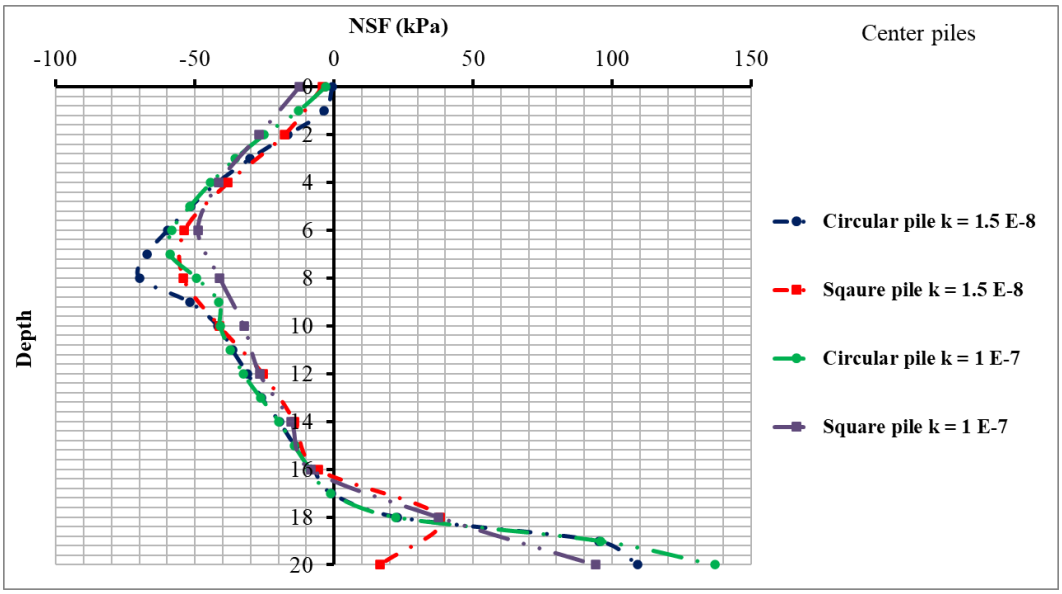

Figure 31. NSF distribution along centre circular piles compared to corner square piles for different values of permeability

Shielding effect was decreased around piles as it goes far from center. Corner pile has the minimum effect. Furthermore, pile geometry effect was clarified as square piles developed slight values of NSF compared with circular piles. Computations also declared that NSF acts in proportional to permeability coefficient of soil (K) as NSF decreased with the decrease of (k) and went to decrease with the reduction of (K). Results of pile groups indicated matching between the behaviour of single piles and piles in groups for the change of soil permeability. NP locations were moving upwards with the increase of (K) as appeared for individual piles.

6.3. Influence of Horizontal Load Value (H) on Circular Piles

Since the study is concentrated on the effect of horizontal load influence on NSF then the amount of the load impacted on piles represents an important factor that should expose the mechanism of lateral movement of the pile under lateral load effect combined with vertical settlement due to consolidation.

In the previous analysis, piles were subjected to horizontal load H = 10 kN. In this section the lateral loads will be increased gradually. The horizontal load will change to be 20, 30, 40, and 50 kN. Single piles will be executed at the beginning of the analysis then an analysis of the pile group will be considered. If the load is increased above 50 kN plastic hinge appeared and the pile failed. Due to the increase in horizontal load intensity, it is expected to have more lateral displacement on soil and pile. This large displacement may cause an increase in compression stress and shear stress inside the soil layer that will enlarge the resistance of the pile (Figure 34).

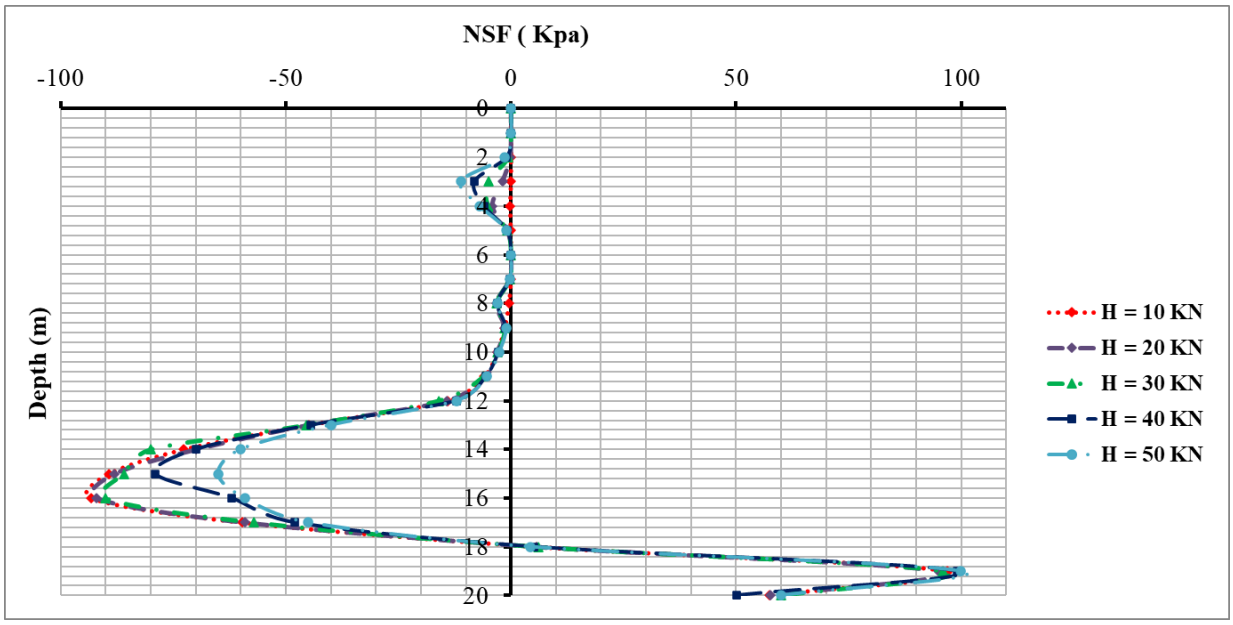

Figure 32. NSF distribution along single circular piles for different values of lateral loads

The distribution of NSF along the pile surface showed that in the upper zone above the location of the plastic hinge NSF is almost zero on the first (2.0 meters) then the NSF values slightly increased the greater the horizontal load the larger the NSF on the pile. This was due to the deformation of the pile which release the pushing force made by the pile on the soil allowing the soil to move downward unrestricted and the shear stress gently affected the pile surface. While in the lower part of the pile the NSF was decreased due to the settlement of soil being decreased when the lateral load was increased. As it was observed when the horizontal load increased the maximum NSF decreased on the surface although it is the small reduction and the difference between the largest and the least was no more than 50 kN.

6.4. Influence of Horizontal Load Value (H) on Square Piles

A change of lateral load value was made for square piles to increase the load gradually from 10 to 50 kN the same as circular piles. Results of single piles were displayed below to compare the NSF distribution for all values of lateral loads.

Figure 35 illustrated the distribution of NSF along 5 individual piles for values of lateral loads starting from 10 kN to 50 kN. Observations of readings lead to deduce that square piles provided NSF less 15% than circular piles. At the top of piles till depth 4.0 m NSF is larger for the load 50 kN and decreased to be minimum for the load 10 kN due to the lateral pressure from the pile into the soil which enlarged the shear stress of soil on the pile surface. When heading downward NSF is reduced slightly small values while the lateral load was increased. The difference in NSF values was not noticeable due to the geometry of the pile. Figure. 31 clarified that square piles dissipated the lateral force along the

pile surface in the downward direction. Almost all lateral had the same maximum point of NSF at the same location on contrary of circular piles. This assumption was supported by settlement values of piles and soil were the same for all values of load.

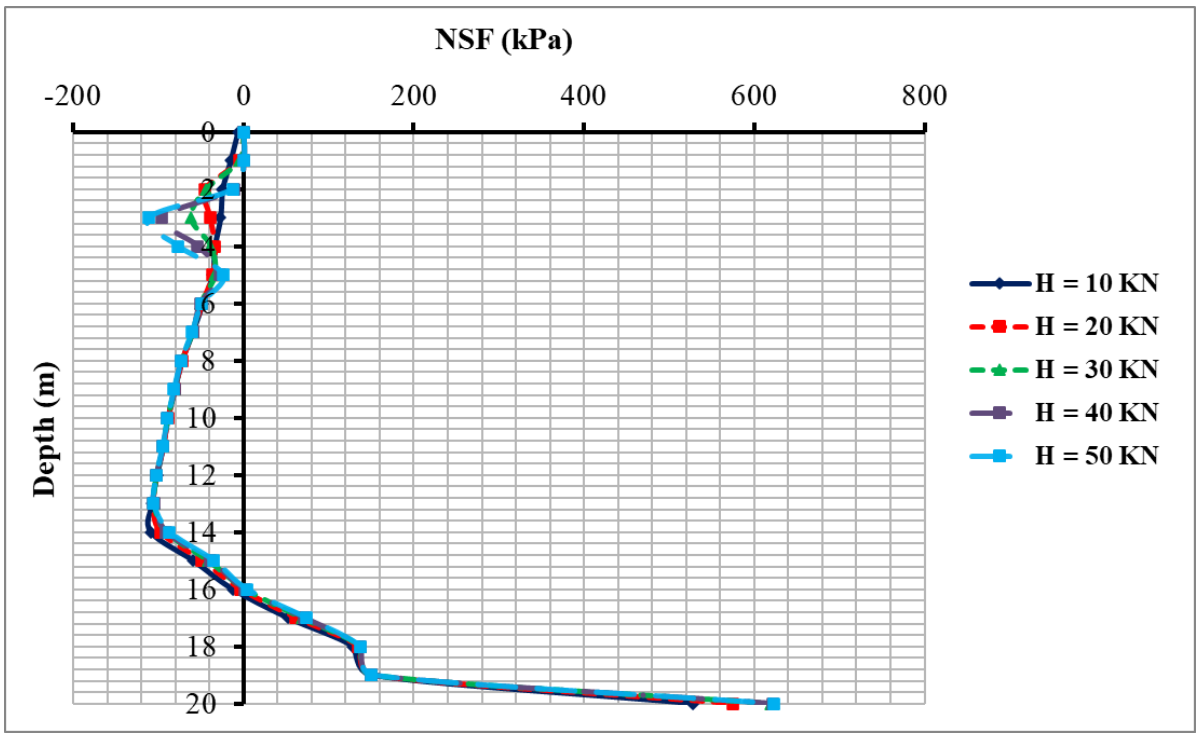

Figure 33. NSF distribution along single square piles for different values of lateral loads

Results of pile groups were displayed to compare the behaviour of circular piles to the square piles according to their positions in the group. Figures 36 and 37 demonstrated NSF distribution along corner piles for circular piles compared to corner square piles in the group for all values of lateral loads.

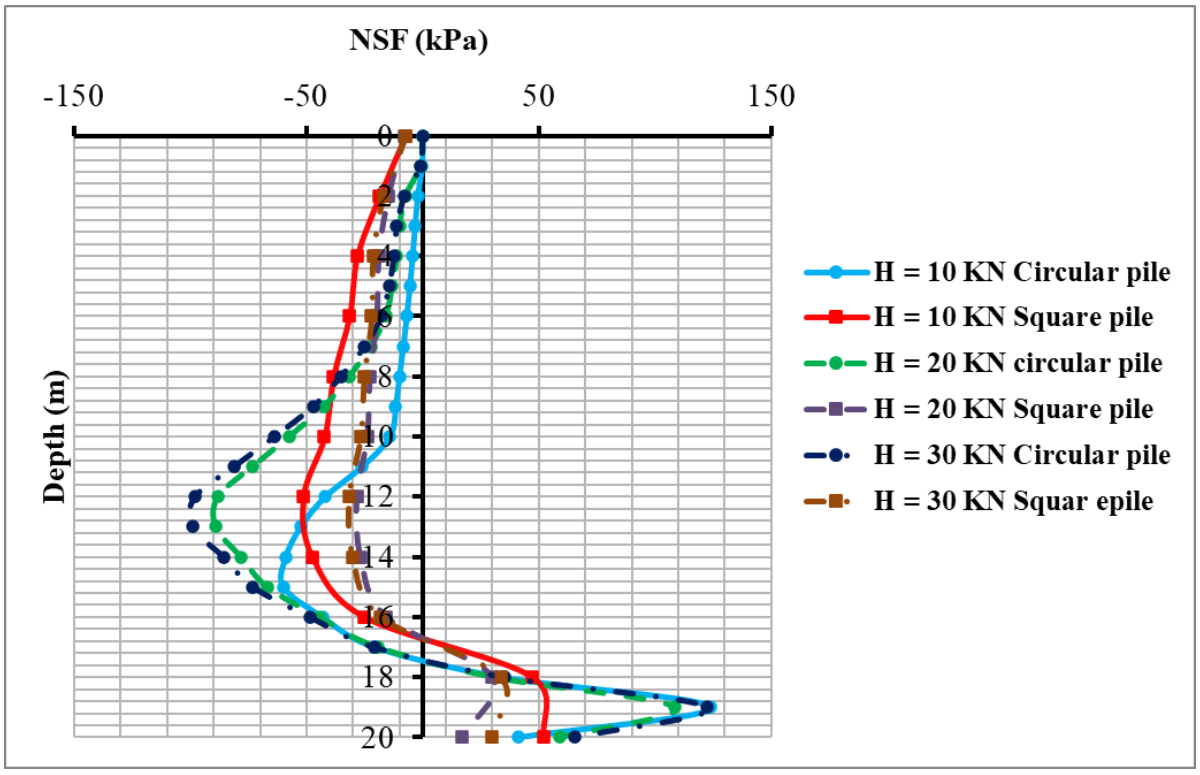

Figure 34. NSF distribution along corner circular piles compared to corner square piles for different values of lateral loads

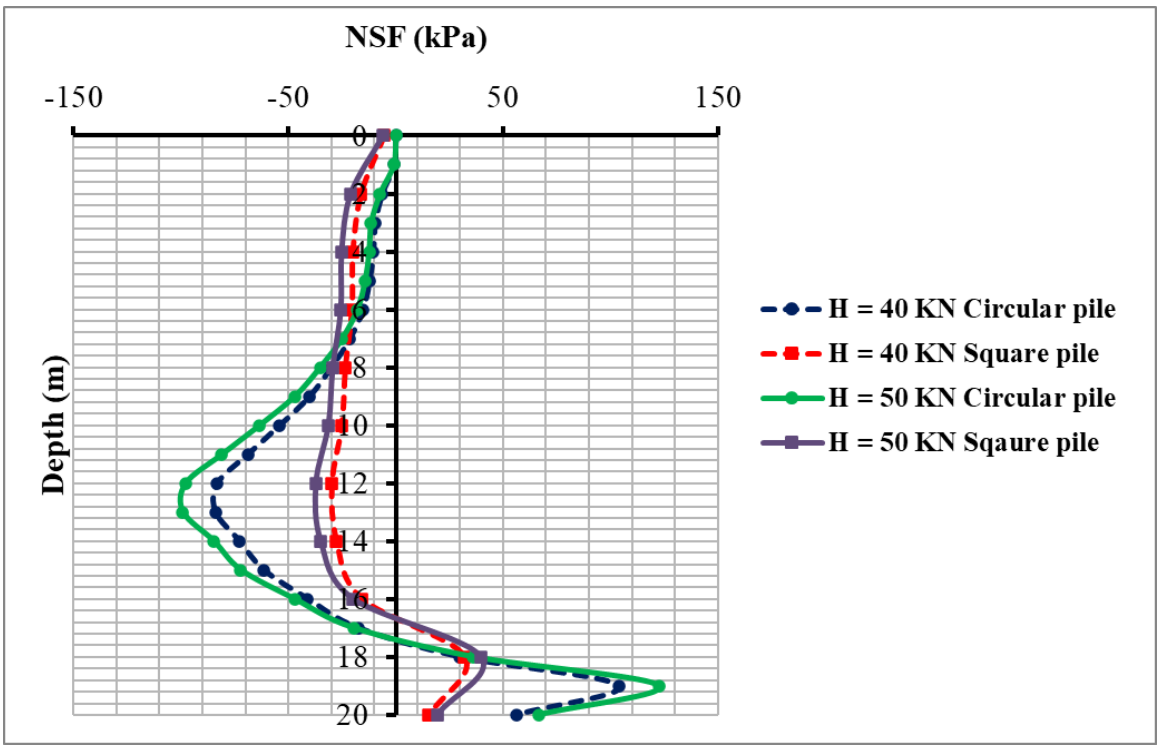

Figure 35. NSF distribution along corner circular piles compared to corner square piles for different values of lateral loads

Readings shown in the Figures determined that NSF developed on the square piles was less than circular piles for all lateral load values but for all values above 10 kN NSF was enlarged 40 % and remained fixed at this limit. The reason for this was that relative displacement between pile and soil was constant for all loads starting from 20 kN. The cause for this unexpected might be the progressive action of the group under lateral loads and the stress interference in zones between piles prevent soil movement downward which reduced the relative settlement. This result implicated that NSF had a limit that could not be exceeded whatever the value of the lateral load acting on the pile. This limit was reached when the pile was loaded with 20 kN. Naturally, this limit of NSF and load value 20 kN will be different according to soil type, dimensions of the pile, surcharge loading on the ground surface, and spacing between piles. The same action appeared for edge piles and corner piles.

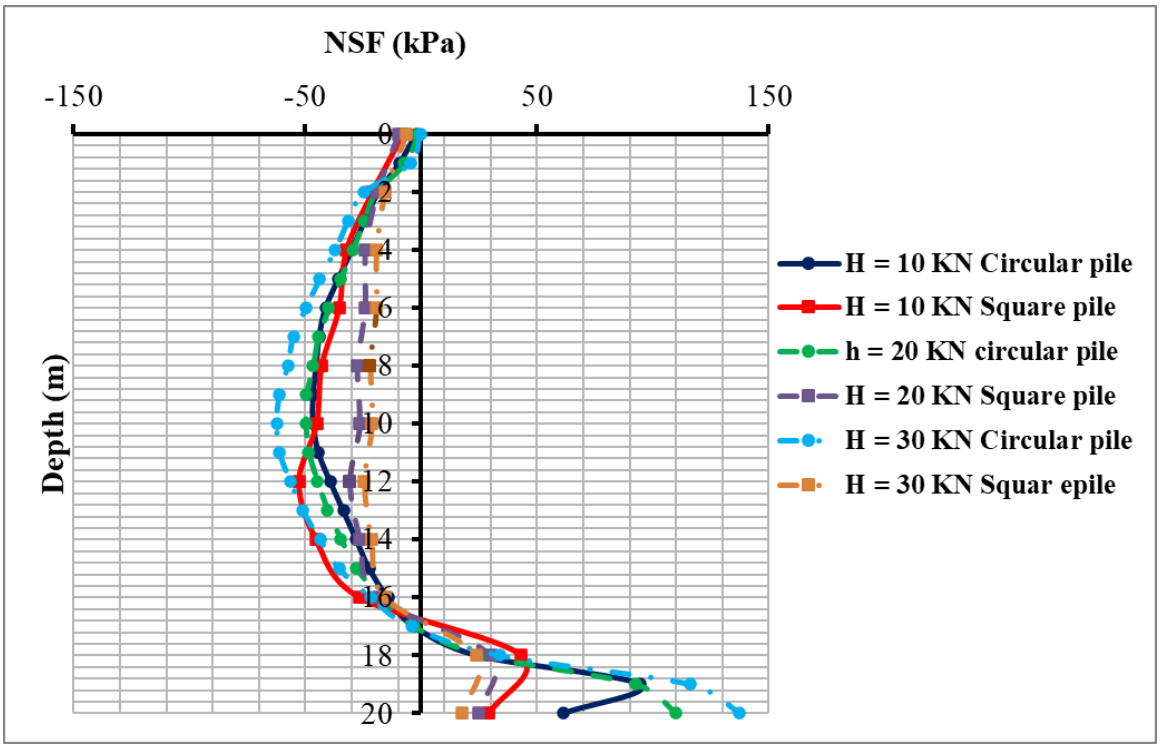

Figure 36. NSF distribution along edge circular piles compared to edge square piles for different values of lateral loads

6.5. Influence of Surcharge Loading Value (q) on Circular Piles

Surcharge loading is the most important factor in the consolidation process. Soil settlement is depending on the surcharge loading during the consolidation and hence surcharge affects indirectly the NSF generated on the pile surface through the soil movement. This part focused on the effect of the horizontal force on the piles subjected to increasing surcharge loading. The conceptual model was run under surcharge = 100 kPa. Gradual increase in the values will take place to use loading = 150, 200, 250 kPa. The horizontal load value is kept constant at 10 kN. The results of the analysis should accentuate how NSF and drag load developed on laterally loaded pile surface under the increase of soil consolidation noting that the consolidation time was kept as 5 years as the conceptual model.

Figure 39 showed that as the surcharge increased the NSF increased in consequence due to the increase of the normal effective stress between the contact surfaces (σ). In addition, the curve showed that horizontal load reduced the values of the NSF on the top part of the pile to zero or particularly petty values then the NSF increased after the influence of the horizontal load is terminated.

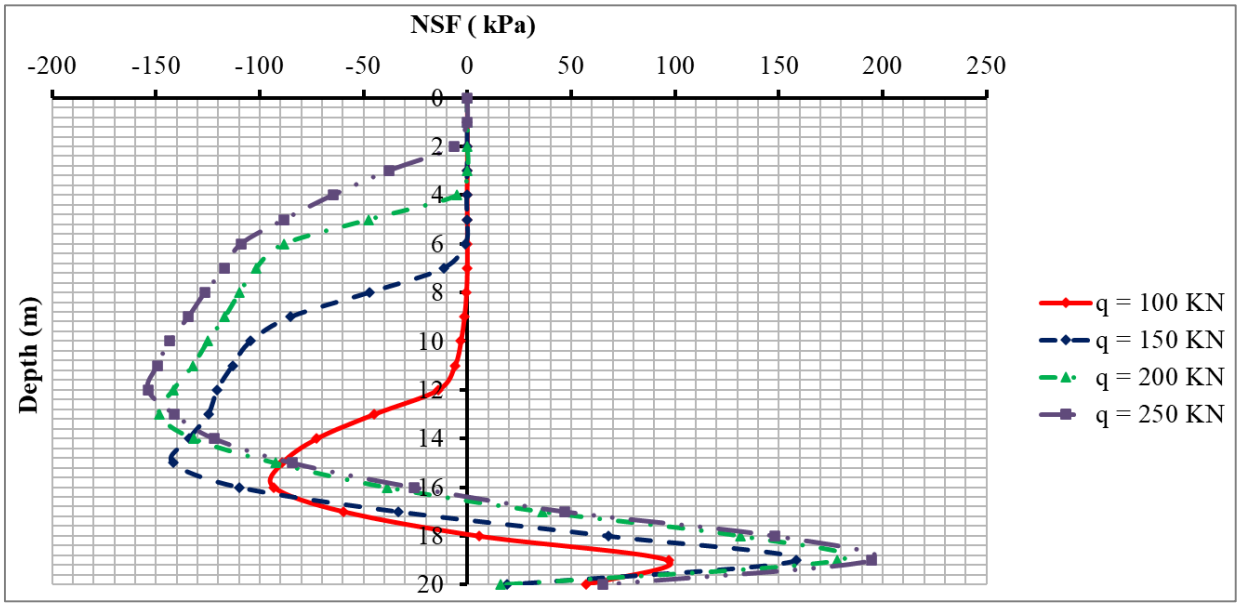

Figure 37. NSF distribution along single circular piles for different values of surcharge loads

Figure 39 spotted that the depth of the pile that is influenced by the horizontal load is extremely affected by the surcharge loading value. When the surcharge increased the depth of influence is decreased and the horizontal load vanished at a higher depth. The increase in the NSF is predicted with the increase in surcharge loading due to the increase in soil settlement. It was noticed that NP location was moving upward as the surcharge load increased and the location of maximum NSF also was moving up due to the limited movement of pile tip for all cases while the soil movement increased with the increase of surcharge.

Verdicts from the curve indicated that increasing surcharge on the ground surface decreased the depth of horizontal load influence on pile surface and the influence of surcharge became greater than horizontal load. Also, a reversal correlation appeared between the NP location and the surcharge load increase. The maximum NSF and drag load did not exhibit a significant difference for surcharge loading 200 kPa and 250 kPa this may indicate that soil has reached the extreme value of the settlement and could not produce more movement.

6.6. Influence of Surcharge Loading Value (q) on Square Piles

The previous surcharge loading pattern was applied again on single square piles. Predictions of results were to find an increase of NSF values with the increase of surcharge loading with remarkable difference proportional with the increase of loading as same as circular piles readings. But NSF results were adjacent with a small increase in values. While in circular piles analysis increase in NSF values was significantly observed it was not noteworthy for square piles. The location of maximum value of NSF was moving upward as the surcharge increased. In addition, the location of NP was observed to be raised with the increase of surcharge load which indicates the increase of PSF zone beneath NP. This movement of NP was expected because NP should reach the point of balance between NSF and PSF (Figure 40).

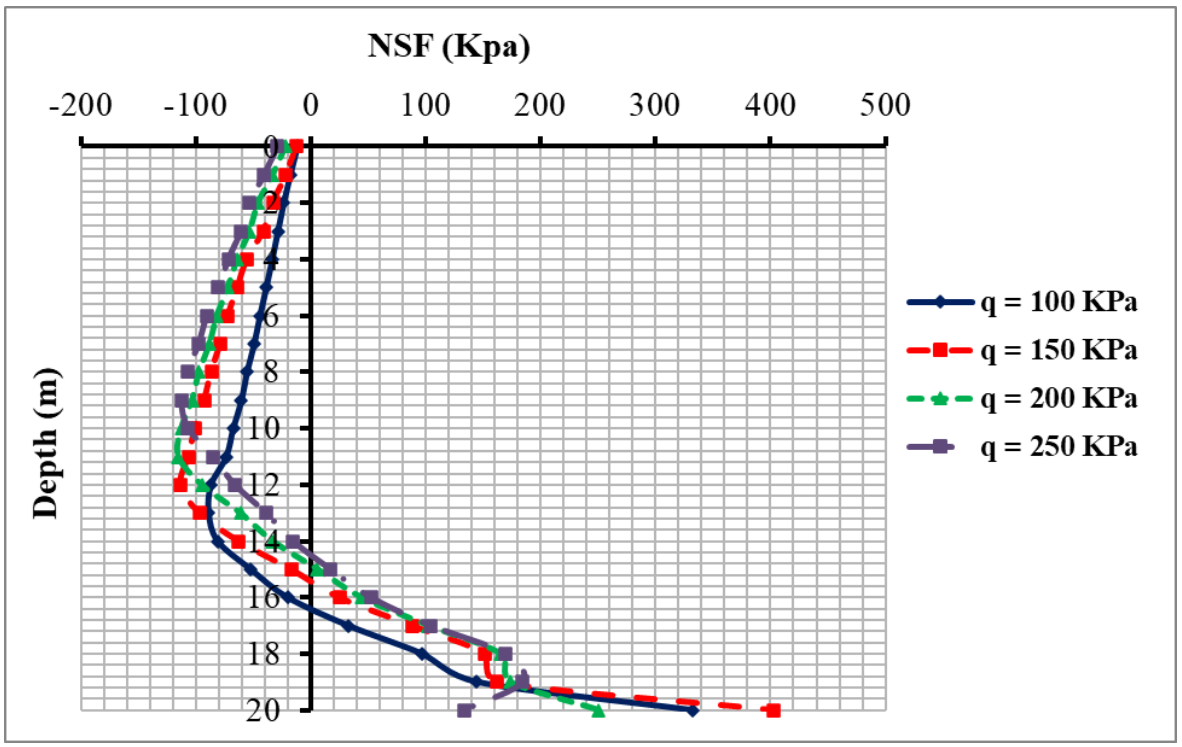

Figure 38. NSF distribution along single square piles for different values of surcharge loads

Readings of pile groups for circular and square piles provided that NSF values on piles in the group were found to be decreased according to the location of piles in the group. The corner pile developed the maximum NSF, the edge pile was the mid value, while the centre pile induced the minimum value of NSF. NSF on square piles was less than NSF developed on the circular piles. For both circular and square pile groups centre piles developed tightly close values with surcharge loads (200 and 250 kPa). Reading of centre piles indicated that the reduction of NSF has reached the certain limit and could not be penetrated whatever the shape of the pile either circular or square as shown in the following Figures 41 to 44.

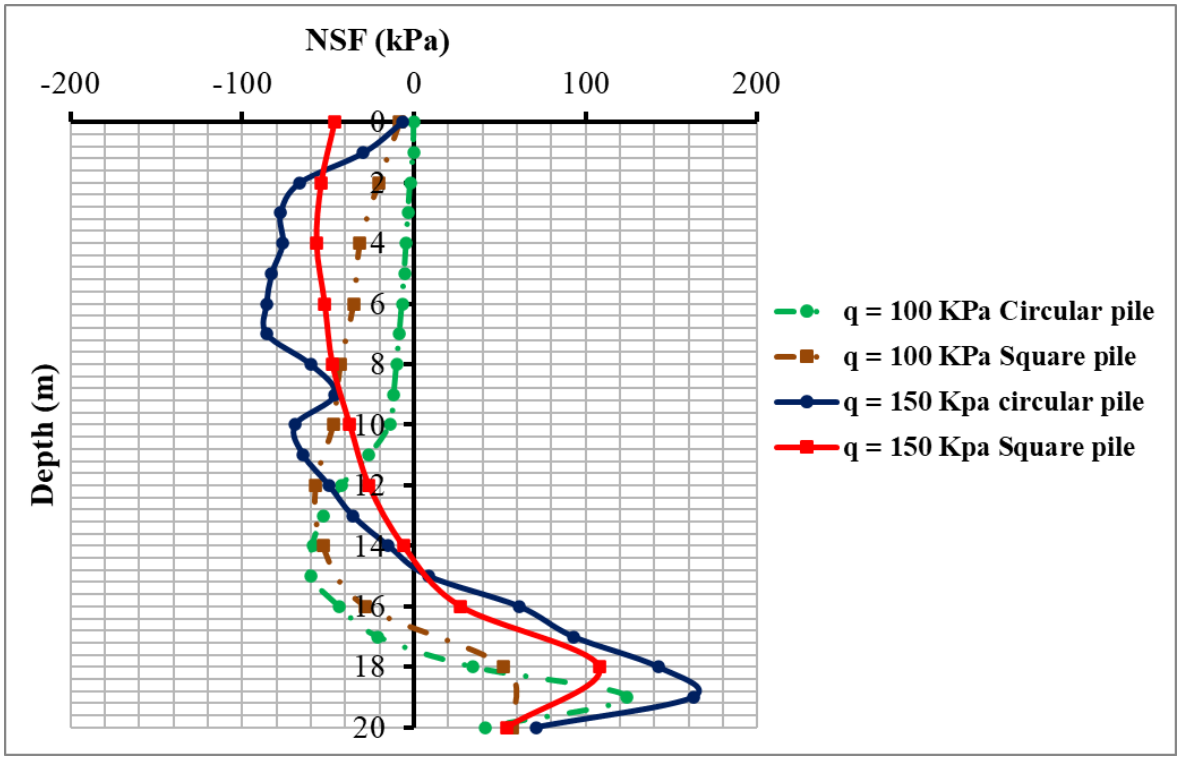

Figure 39. NSF distribution along corner circular piles compared to corner square piles for different values of surcharge loads

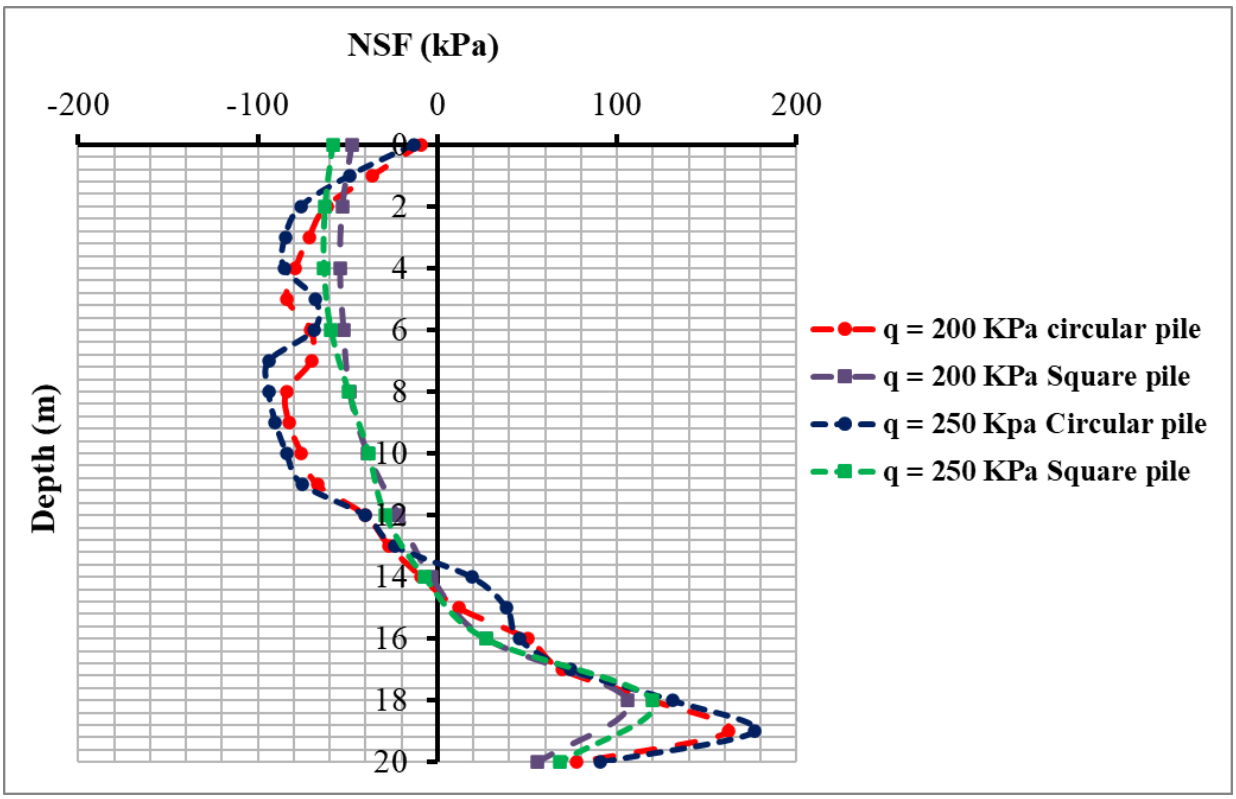

Figure 40. NSF distribution along corner circular piles compared to corner square piles for different values of surcharge loads

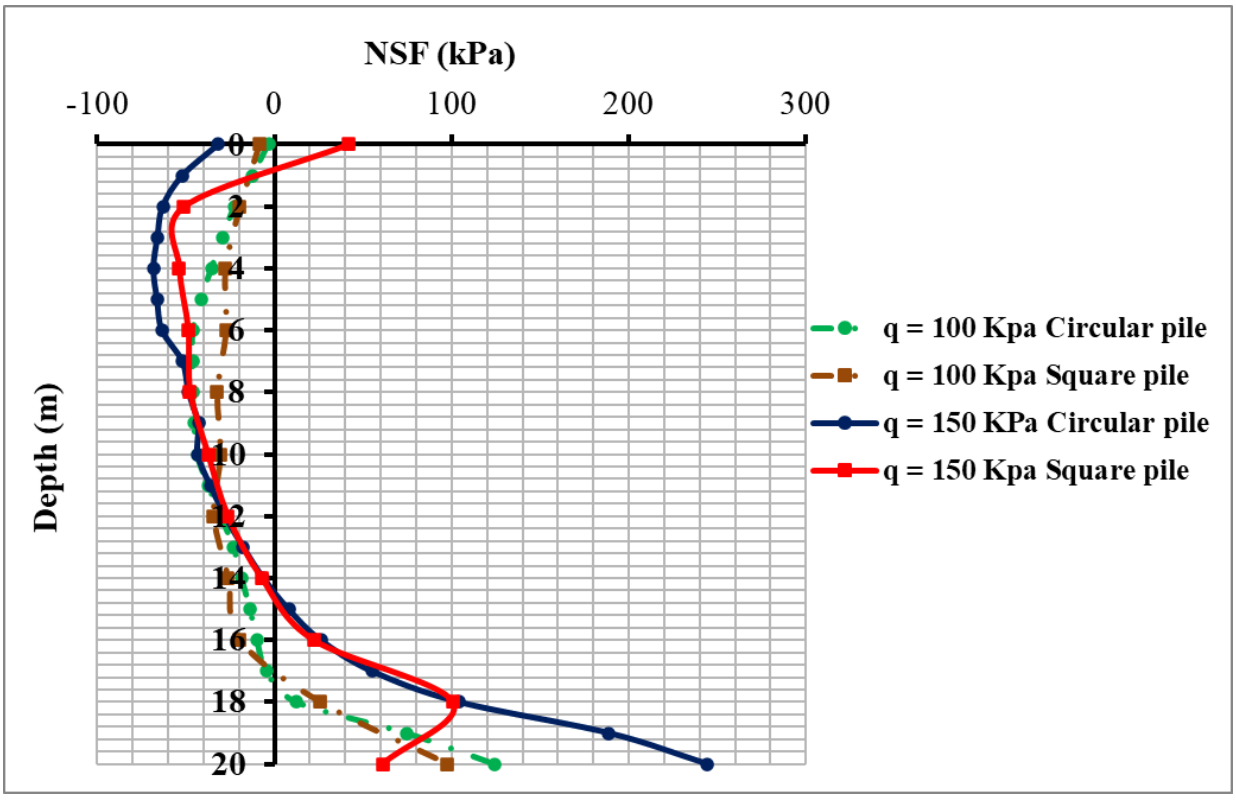

Figure 41. NSF distribution along centre circular piles compared to centre square piles for different values of surcharge loads

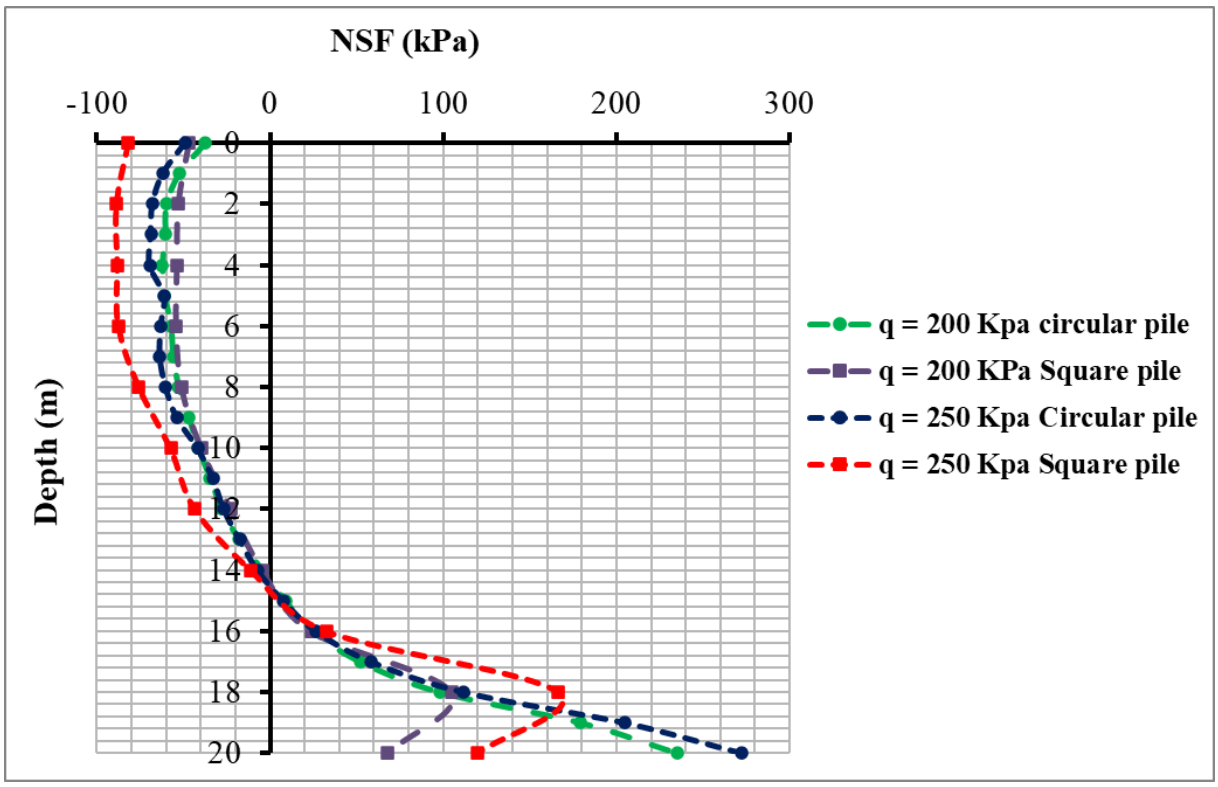

Figure 42. NSF distribution along centre circular piles compared to centre square piles for different values of surcharge loads

6.7. Influence of Eccentricity on Circular Piles

In all previous models, piles were created as free head piles (without pile cap). The top of the pile was levelled with the ground top surface. This condition does not allow comprising bending moment over the pile.

This clause is dedicated to investigating the influence of bending moment on pile NSF due to eccentricity. Eccentricity will be formed when extending the pile top out above the ground surface. A distance (e = 0.5 m) was chosen to be extended above the ground surface. Hence the resulted bending moment will be H × e = 10 × 0.5 = 5 kN.m = 5000 N.m (Figure 45).

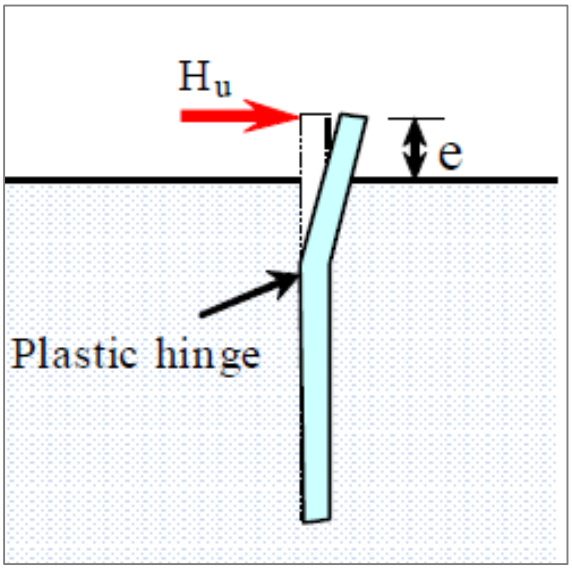

Figure 43. Eccentricity of pile above the ground surface

It was aimed to investigate the influence of the resulted rotation of pile due moment on the developed NSF and drag load compared to the one without eccentricity because this geometry of piles is considered the closest approach to the construction of piles on site.

Figure 46 illustrated the results of the analysis of the pile subjected to eccentricity. The NSF on the upper part was zero for the first 5 meters. Then it increased to be larger than the one without eccentricity with 10 kN. That increase in NSF was due to the rotation of the pile which indicated that rotation affected the pile movement and decreased the settlement of the pile while the soil settlement did not change which is reflected on the enlargement of NSF value due to the increase of relative displacement between pile and soil as shown in Figure 47.

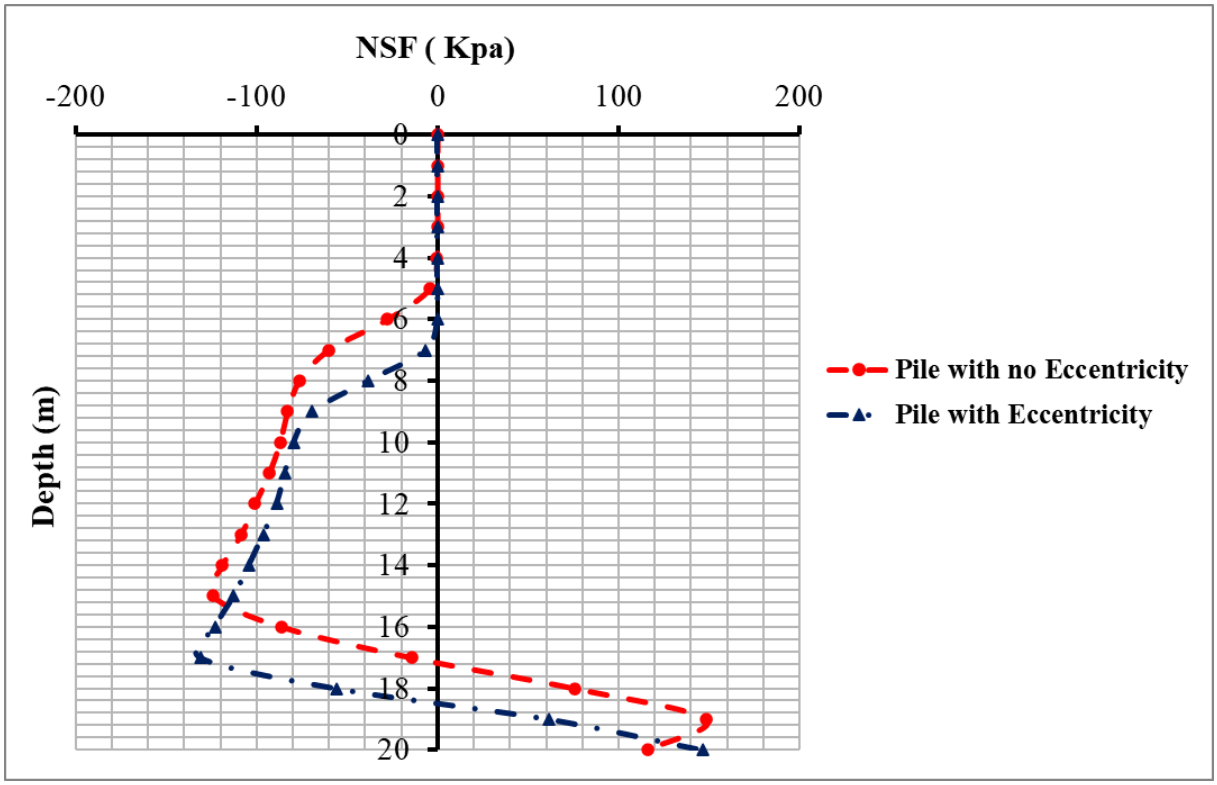

Figure 44. Distribution of NSF along laterally loaded circular single pile with and without eccentricity on the pile

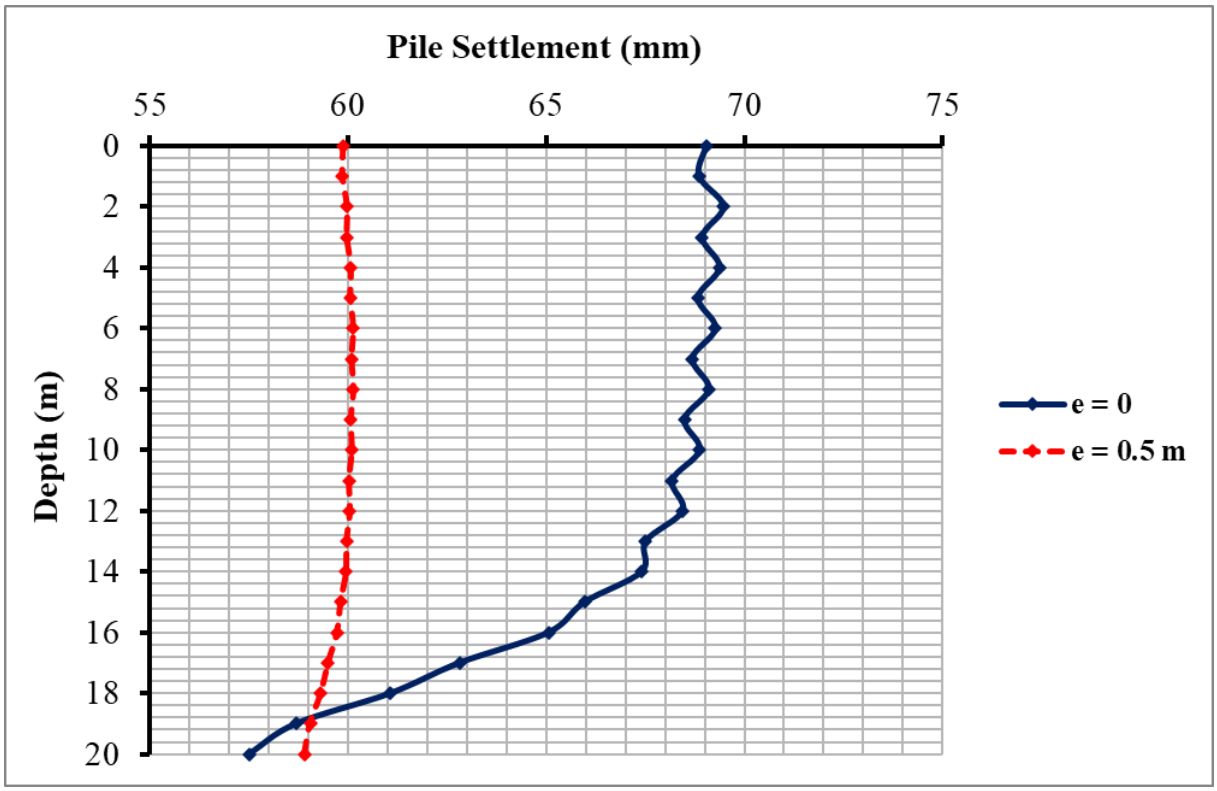

Figure 45. Pile settlement for laterally loaded single pile with eccentricity and without eccentricity

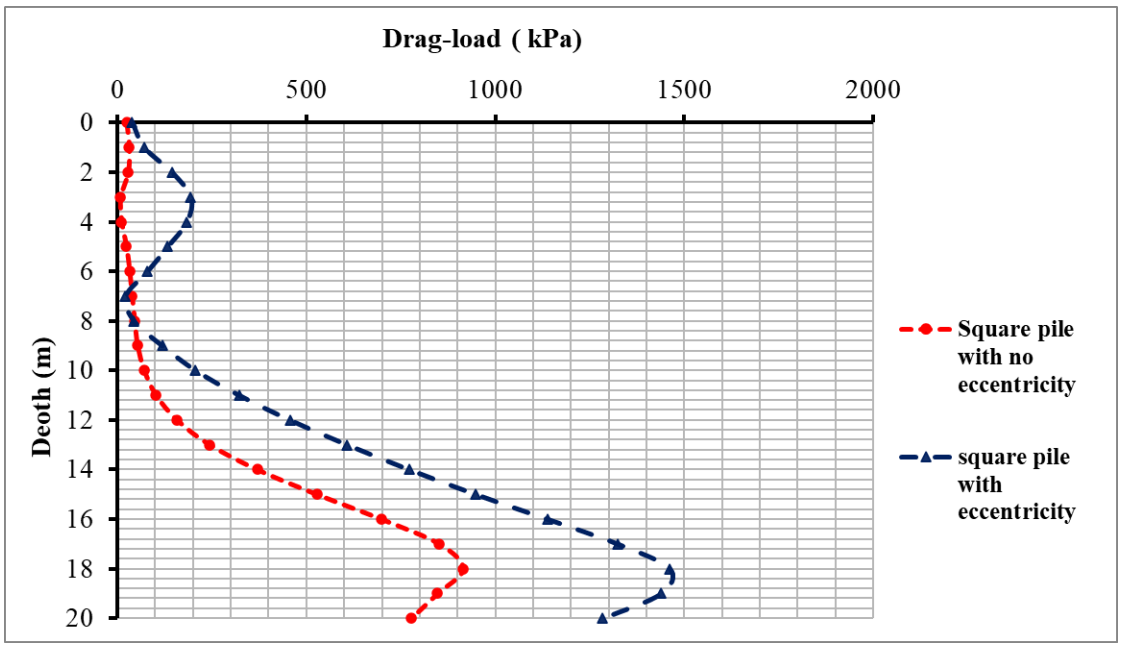

Figure 46. Pile Drag load on the circular single pile with eccentricity against pile without eccentricity

Drag load on the pile showed that an increase at the top of the pile till the location of the expected plastic hinge that would be formed when the moment exceeded the pile capacity (Figure 48). Then it decreased to reach the minimum value at depth 7.0 m and then increased again to reach the maximum value which is larger than the pile without eccentricity. That behaviour was due to the bending moment generated on the pile as it increased the compression axial load on the pile and increased the drag load at the top. The drag load at the NP location matched the behaviour of NSF on the pile to exceed the maximum NSF for the other pile.

6.8. Influence of Eccentricity on Square Piles

An extension of the pile (e = 0.5 m) was created on the square pile to investigate the eccentricity effect on the square pile. Comparison between the cases of loading showed that eccentricity on the pile slightly increased the NSF developed on the pile surface. The particular reason for that was due to pile and soil settlements. They were very close in the two cases and the difference did not allow to development of large NSF for the eccentric pile. NP location moved a little bit upward as shown in Figure 49.

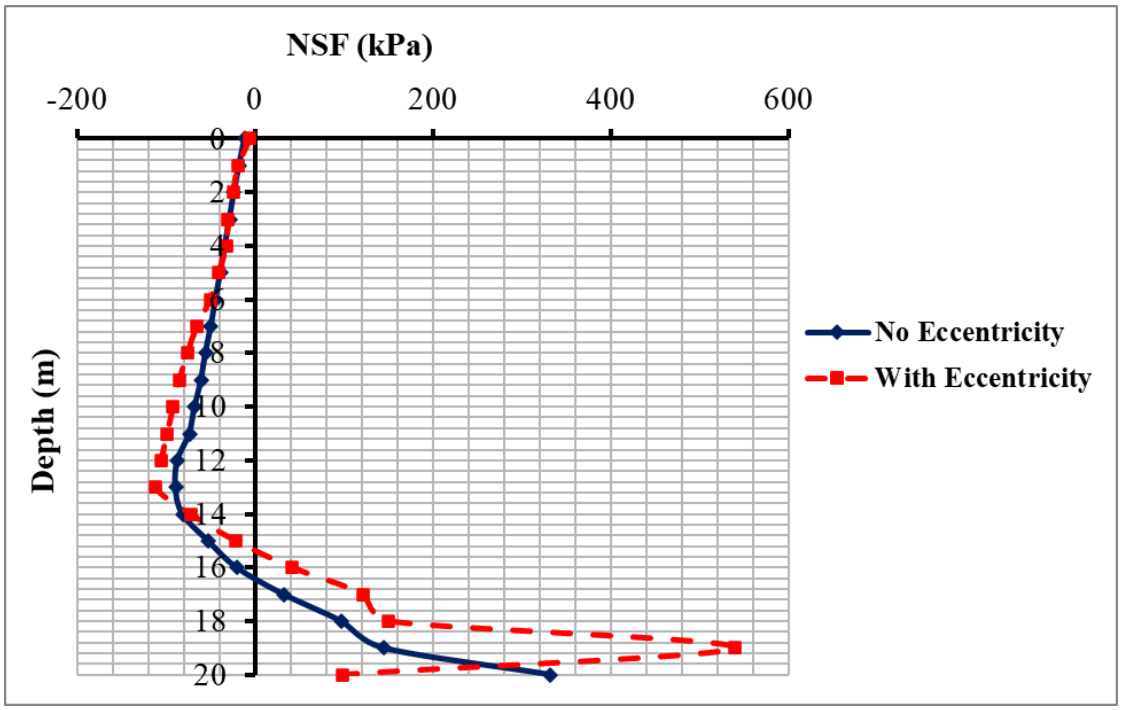

Figure 47. Distribution of NSF along laterally loaded square single pile with and without eccentricity on the pile

Comparison between the NSF along eccentric load circular pile against eccentric laterally loaded square pile illustrated in Figure 50 indicated that the square pile was slightly less than the circular pile. The difference between the two piles was 18 kPa. The reason for that was the bending moment acted on both piles. When piles rotated inside the soil layer, they prevented the soil from settling in a full range which caused small relative displacement between soil and pile for both piles.

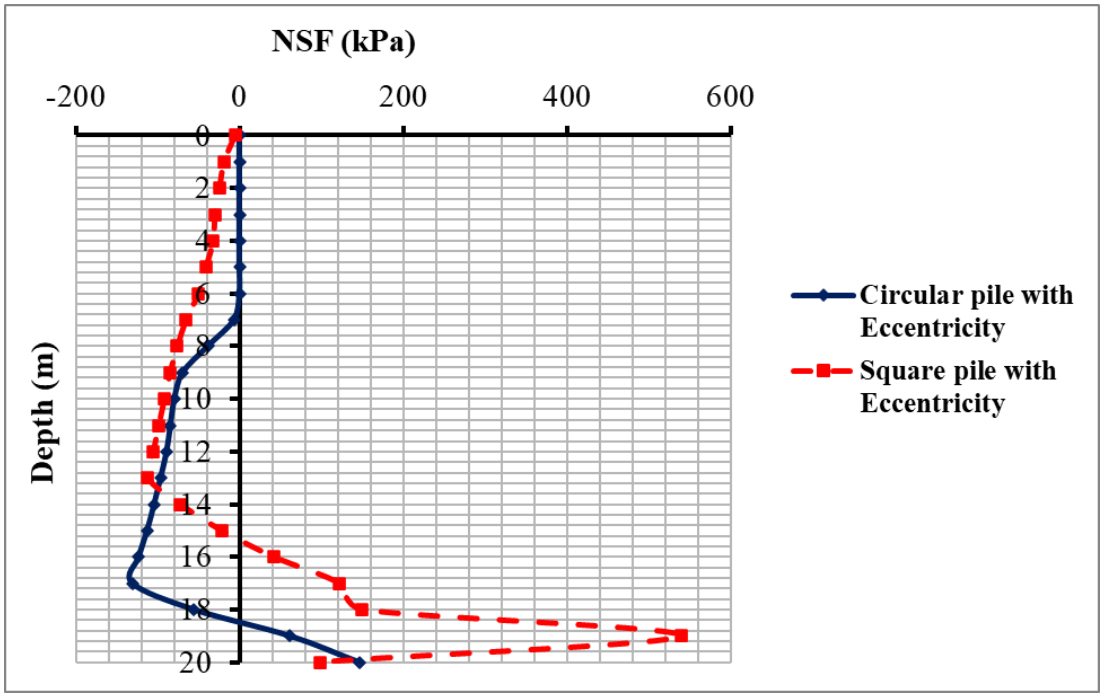

Figure 48. Distribution of NSF along eccentric load circular pile against the eccentric laterally loaded square pile

The same behaviour of single piles can be observed in group analysis when comparing centre piles NSF values as shown in Figure 51 as a result of the grouping action these centre piles were considered the most protected piles in the groups and they developed the minimum NSF.

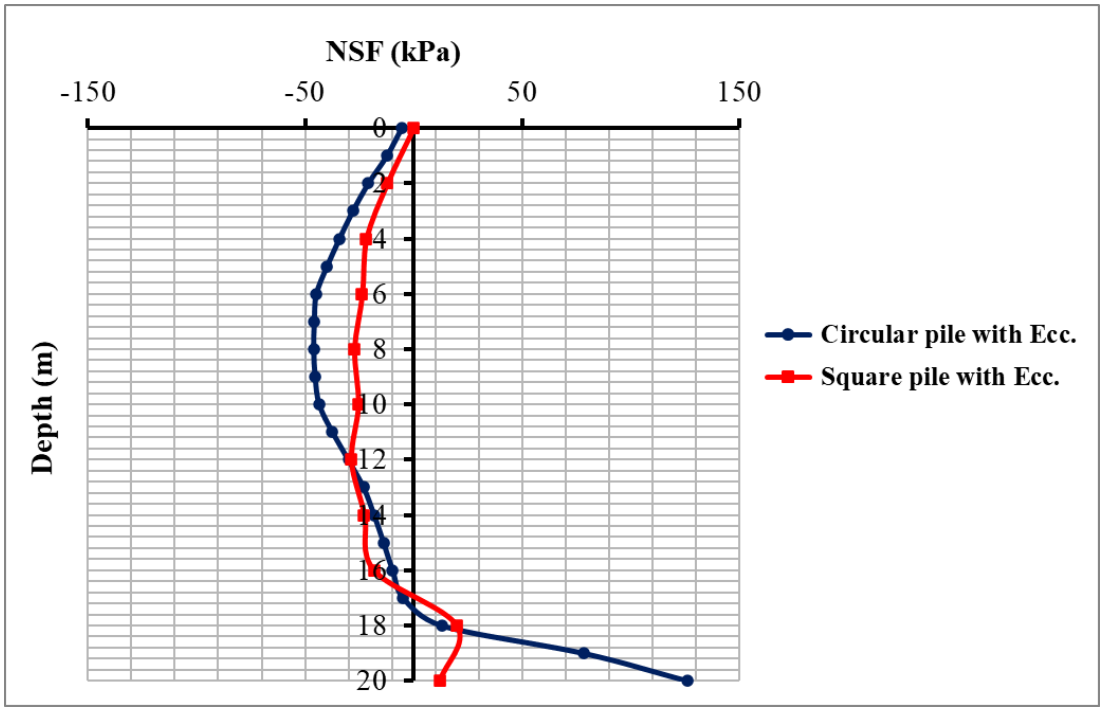

Figure 49. Distribution of NSF along centre circular pile compared to centre square pile subjected to eccentricity

Corner piles and edge piles developed more larger NSF along piles surfaces and the difference between the circular pile and the square pile was significantly large. Stress interference around the piles was the direct cause of these readings.

Interference of stress increased the soil settlement which caused an increase in the NSF induced along corner piles surfaces but square piles preserved their condition and provided less stress than a circular piles (Figure 52 and 53).

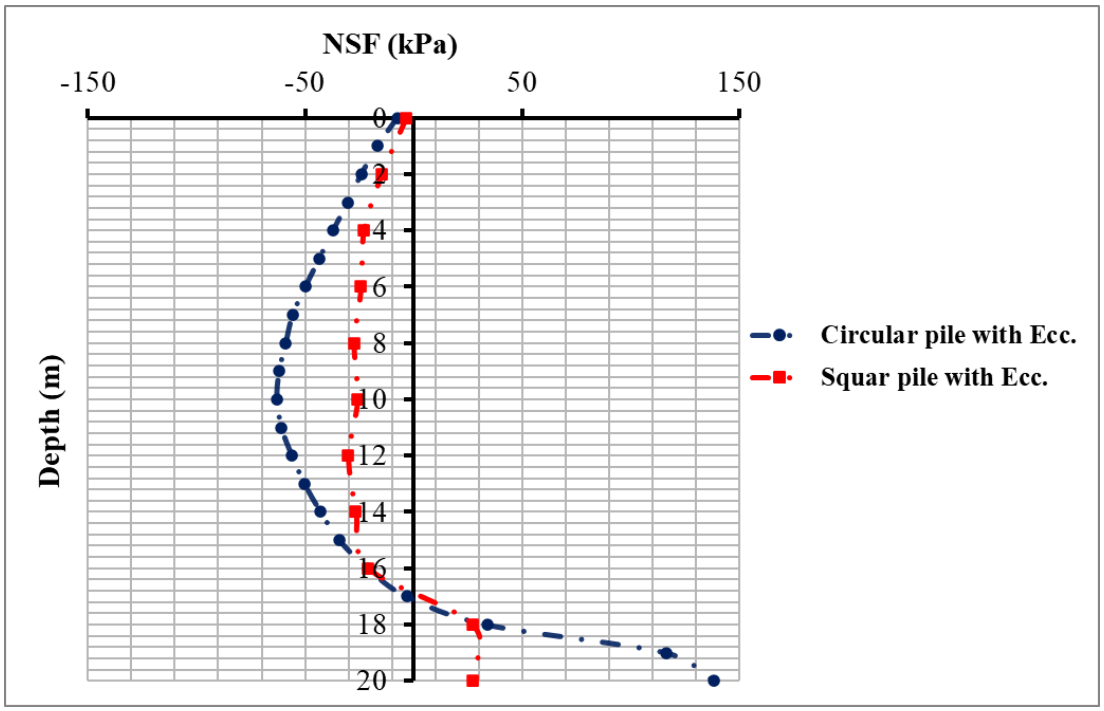

Figure 50. Distribution of NSF along edge circular pile compared to edge square pile subjected to eccentricity

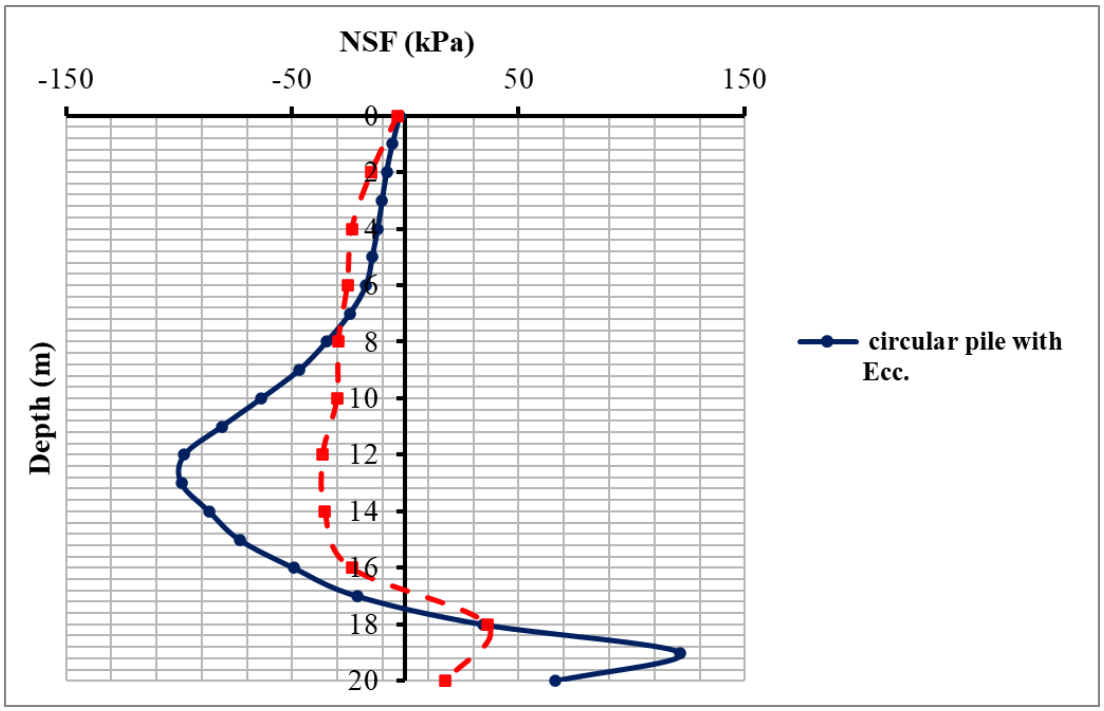

Figure 51. Distribution of NSF along corner circular pile compared to corner square pile subjected to eccentricity

7. Conclusions

This search was dedicated to numerically investigating the effect of changing the shape of the pile from circular to square shape on the values of NSF developed on both of them due to soil consolidation for a period of 5 years. Also, it investigated the influence of pile lateral load on the behaviour of NSF of piles installed in soft clay. ABAQUS software was used to model the simulation of piles and soil with FEM.

The objective was divided into three paths, first was to check if the NSF developed on the pile may be reduced when the geometry of the pile changed to square keeping the same cross-section area. The second was to detect whether the

horizontal load on piles has any effect on the NSF and drag load. In the end, we compared the behaviour of the piles in groups to recognize the behaviour of NSF on both circular and square piles for soil parameters such as interface friction coefficient and soil permeability, then the lateral load value was increased gradually on the pile, and finally the surcharge loading causing consolidation process over the ground surface was increased from 100 to 250 KPa with a constant step of 50 KPa.

The numerical analysis provided the following conclusions:

- The outcomes of the analysis for the square piles showed a large reduction in values of NSF compared to circular piles with an equivalent perimeter along the pile surface. This emphasizes the core idea of the study that change geometry of pile can enhance the NSF and the ability to replace the coating concept with transforming the circular pile into square pile to obtain better behaviour of NSF on pile.
- Piles subjected to lateral loads generated NSF values were significantly less than NSF values induced along the piles without lateral load which leads to new spot on the design of laterally loaded piles to use lateral loads as a reduction factor of NSF.
- The interface friction coefficient plays a great role in forming NSF on the pile side. The effect of the interface friction coefficient is similar on both circular and square piles. Analysis results illustrated that a large value of the interface friction coefficient provided large values of NSF on the pile surface. NSF decreased with the decrease of friction coefficient value. When comparing square piles and circular piles, it was clear that square piles provided better NSF values along the pile side.
- Soil permeability was found to have a delicate effect on the NSF. When the permeability coefficient value increased, soil settlement increased, and as a consequence, NSF increased along the pile surface for both square and circular piles. The values of NSF generated on square piles were slightly smaller than those on circular piles.
- Lateral load value enlargement has a reverse relationship with NSF on circular piles, while on square piles the effect was not significant as square piles showed high resistance to the displacement under all values of lateral loads.

8. Declarations

8.1. Author Contributions

Conceptualization, O.SH. and A.T.; methodology, M.M.; software, O.SH.; validation, O.SH., A.T. and M.M.; formal analysis, O.SH.; investigation, A.T.; resources, O.SH.; data curation, O.SH.; writing—original draft preparation, O.SH.; writing—review and editing, A.T.; visualization, M.M.; supervision, M.M.; project administration, M.M. All authors have read and agreed to the published version of the manuscript.

8.2. Data Availability Statement

The data presented in this study are available in the article.

8.3. Funding

The authors received no financial support for the research, authorship, and/or publication of this article.

8.4. Conflicts of Interest

The authors declare no conflict of interest.

9. References

[1] Fellenius, B. H. (1988). Unified design of piles and pile groups. Transportation Research Record, 1169, 75–82.

[2] Indraratna, B., Balasubramaniam, A. S., Phamvan, P., & Wong, Y. K. (1992). Development of negative skin friction on driven piles in soft Bangkok clay. Canadian Geotechnical Journal, 29(3), 393–404. doi:10.1139/t92-044.

[3] Abdrabbo, F. M., & Ali, N. A. (2015). Behaviour of single pile in consolidating soil. Alexandria Engineering Journal, 54(3), 481–495. doi:10.1016/j.aej.2015.05.016.

[4] Muni, T., Devi, D., & Baishya, S. (2021). Parametric Study of Sheet Pile Wall using ABAQUS. Civil Engineering Journal, 7(1), 71-82. doi:10.28991/cej-2021-03091638.

[5] Chen, R. P., Zhou, W. H., & Chen, Y. M. (2009). Influences of soil consolidation and pile load on the development of negative skin friction of a pile. Computers and Geotechnics, 36(8), 1265–1271. doi:10.1016/j.compgeo.2009.05.011.

[6] Chan, S. H. (2006). Negative Skin Friction on Piles in Consolidation Ground. Master Thesis, Hong Kong University of Science and Technology, Clear Way Bay, Hong Kong.

[7] Abo-Youssef, A., Morsy, M. S., ElAshaal, A., & El-Mossallamy, Y. M. (2021). Numerical modelling of passive loaded pile group in multilayered soil. Innovative Infrastructure Solutions, 6(2), 1-13. doi:10.1007/s41062-021-00464-6.

[8] Feng, Z., Hu, H., Zhao, R., He, J., Dong, Y., Feng, K., Zhao, Y., & Chen, H. (2019). Experiments on reducing negative skin friction of piles. Advances in Civil Engineering, 2019. doi:10.1155/2019/4201842.

[9] Zhang, Z., Rao, F. R., & Ye, G. B. (2020). Design method for calculating settlement of stiffened deep mixed column-supported embankment over soft clay. Acta Geotechnica, 15(4), 795–814. doi:10.1007/s11440-019-00780-3.

[10] Alipour, R., Khazaei, J., Pakbaz, M. S., & Ghalandarzadeh, A. (2017). Settlement control by deep and mass soil mixing in clayey soil. Proceedings of the Institution of Civil Engineers: Geotechnical Engineering, 170(1), 27–37. doi:10.1680/jgeen.16.00008.

[11] Pakbaz, M. S., & Alipour, R. (2012). Influence of cement addition on the geotechnical properties of an Iranian clay. Applied Clay Science, 67–68, 1–4. doi:10.1016/j.clay.2012.07.006.

[12] Hajitaheriha, M. M., Jafari, F., Hassanlourad, M., & Hasani Motlagh, A. (2021). Investigating the reliability of negative skin friction on composite piles. Civil Engineering Infrastructures Journal, 51(1), 23–42. doi:10.22059/CEIJ.2020.287489.1607.

[13] Hajitaheri Ha, M. M., & Hassanlourad, M. (2015). Numerical modeling of the negative skin friction on single vertical and batter pile. Acta Geotechnica Slovenica, 12(2), 47-55.

[14] Zhao, Z., Ye, S., Zhu, Y., Tao, H., & Chen, C. (2022). Scale model test study on negative skin friction of piles considering the collapsibility of loess. Acta Geotechnica, 17(2), 601–611. doi:10.1007/s11440-021-01254-1.

[15] shawky, O., Altahrany, A. I., & Elmeligy, M. (2022). Improved Pile Geometry to Reduce Negative Skin Friction on Single Driven Pile and Pile Groups Subjected to Lateral Loads. Geotechnical and Geological Engineering, 40(9), 4487–4516. doi:10.1007/s10706-022-02165-y.

[16] ABAQUS. (2014) Abaqus 6.14 Analysis User's Guide. ABAQUS Inc. Johnston, Rhode Island, United States.

[17] Lee, C. J., & Ng, C. W. W. (2004). Development of Downdrag on Piles and Pile Groups in Consolidating Soil. Journal of Geotechnical and Geoenvironmental Engineering, 130(9), 905–914. doi:10.1061/(asce)1090-0241(2004)130:9(905).

[18] Savvides, A. A., & Papadrakakis, M. (2022). Uncertainty Quantification of Failure of Shallow Foundation on Clayey Soils with a Modified Cam-Clay Yield Criterion and Stochastic FEM. Geotechnics, 2(2), 348-384. doi:10.3390/geotechnics2020016.

[19] Randolph, M. F., & Wroth, C. P. (1978). Analysis of Deformation of Vertically Loaded Piles. Journal of the Geotechnical Engineering Division, 104(12), 1465–1488. doi:10.1061/ajgeb6.0000729.

[20] El-Meligy, M. M., Mahmoud, A. I., & Mohamed, S. M. (2016). Studying the Effect of Pile-Soil Interface Properties on Piles Subjected to Negative Skin Friction. New York Science Journal, 9(3), 103–115. doi:10.7537/marsnys09031617.

[21] Potyondy, J. G. (1961). Skin friction between various soils and construction materials. Geotechnique, 11(4), 339–353. doi:10.1680/geot.1961.11.4.339.

[22] Yao, W., Liu, Y., & Chen, J. (2012). Characteristics of Negative Skin Friction for Superlong Piles under Surcharge Loading. International Journal of Geomechanics, 12(2), 90–97. doi:10.1061/(asce)gm.1943-5622.0000167.